Graphene-decorated photonic waveguide devices

- Motivation
- Surface conductivity of graphene
- Graphene on a planar waveguide
- Graphene in classical electrodynamics:
  - Boundary condition
  - “Volumetric” approach
    - Role of “background permittivity”
  - Perturbation approach
- Graphene surface plasmons
- Ribbon plasmons & extraordinary reflection from the boundary
- Coupling of graphene surface plasmons with guided mode
- ???

Motivation

Graphene monolayer – an iconic representant of 2D materials – has introduced a new challenge also in the field of numerical simulations of photonic devices.

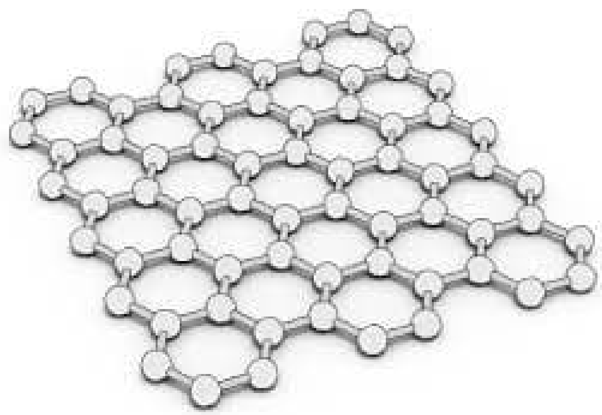

Monolayer thickness: O (0.1 nm)

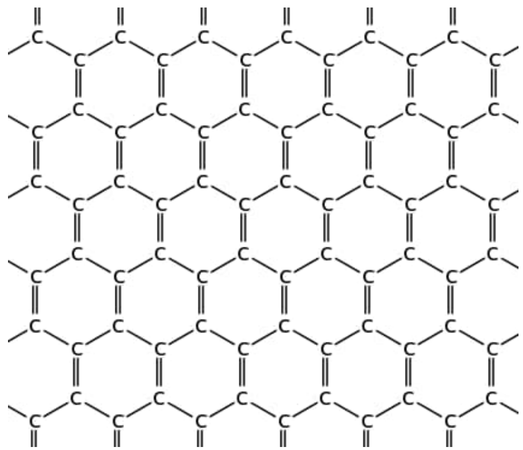

Inter-atomic distance: 0.142 nm

How to characterize 2D materials within the frame of a classical electrodynamics?
For VIS-NIR photonics ($\lambda \approx 1\ \mu\text{m}$): *sheet conductivity of an "infinitely thin" layer*

Motivation

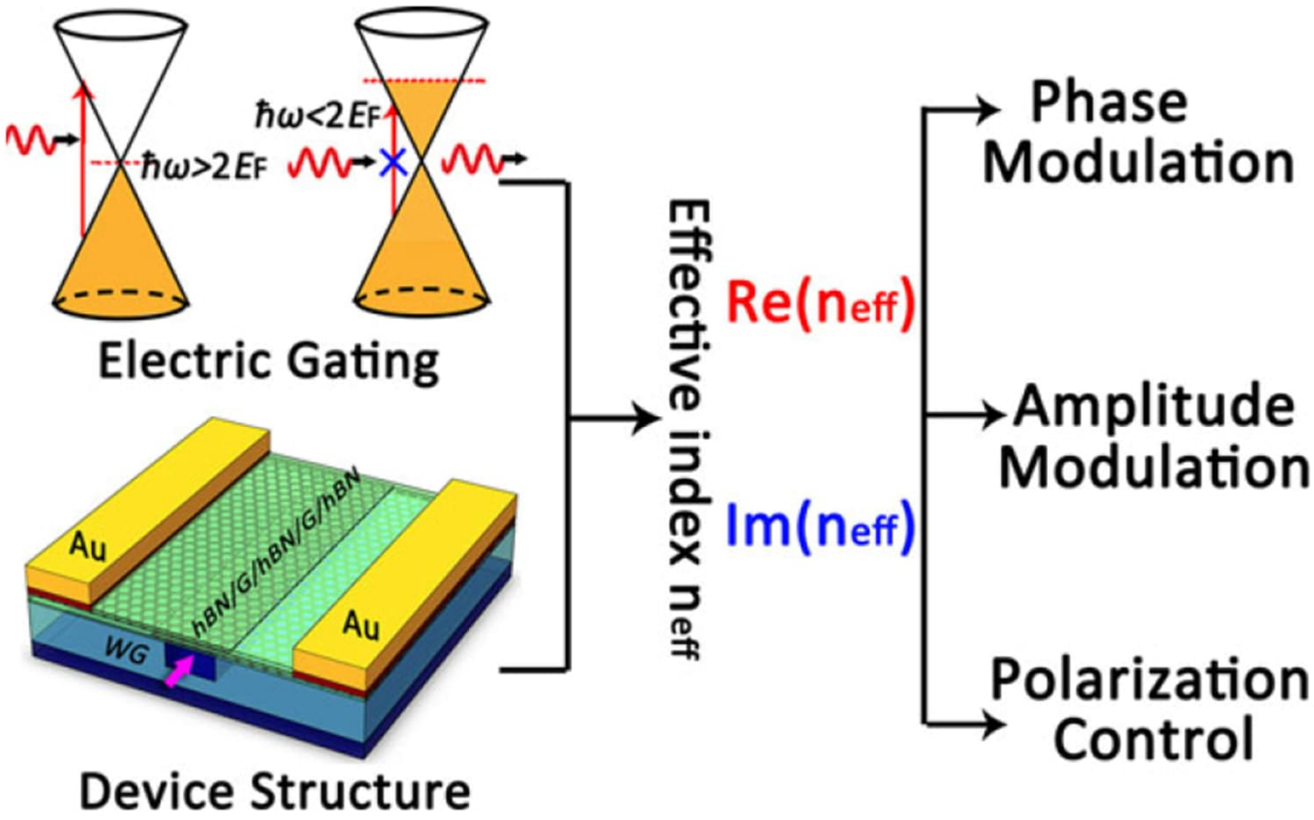

Meng Y, Ye SW, Shen YJ, Xiao QR, Fu X, Lu RG, et al. Waveguide Engineering of Graphene Optoelectronics-Modulators and Polarizers. IEEE Phot J. 2018;10(1):6600217.

Electro-optic modulators with single and double graphene layer

Tao Y. et al., , Opt Express, 27(6), 9013-31, 2019.

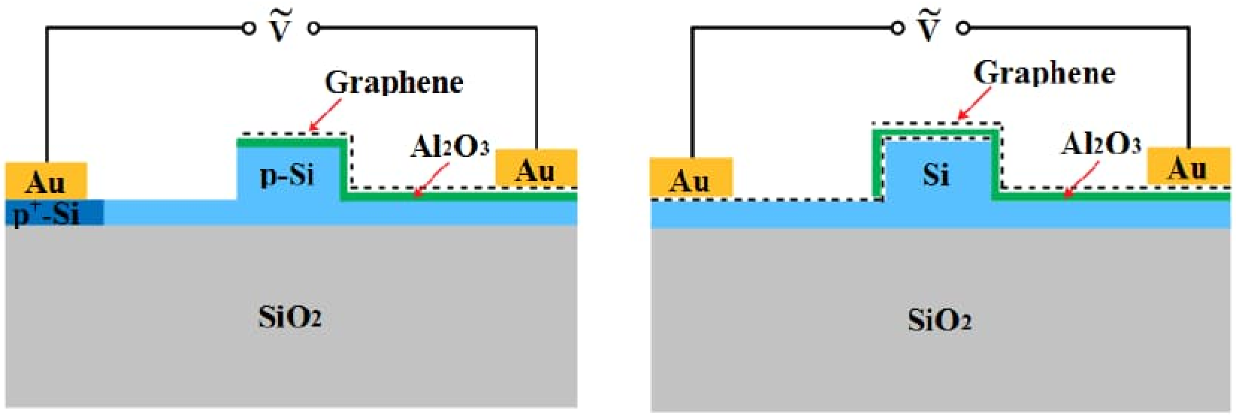

Optical switching through graphene-induced exceptional points

Chatzidimitriou D, Kriezis EE., JOSA B, 35(7), 1525-35, 2018.

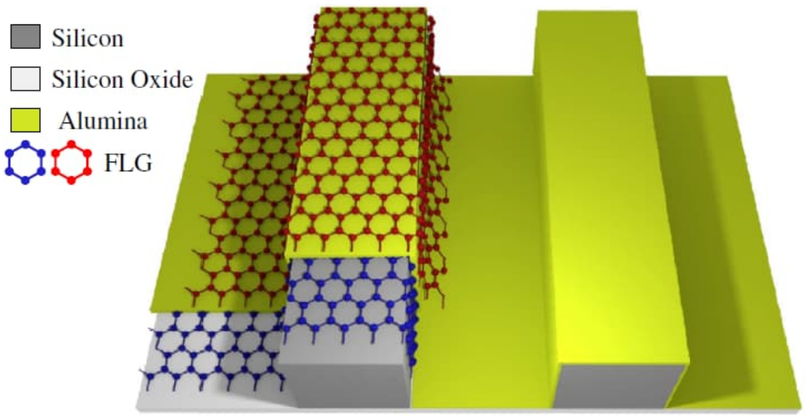

quasi-*PT* symmetric structure
without gain

Kovacevic G. et al., Applied Physics Express, 11(6), 065102, 2018.

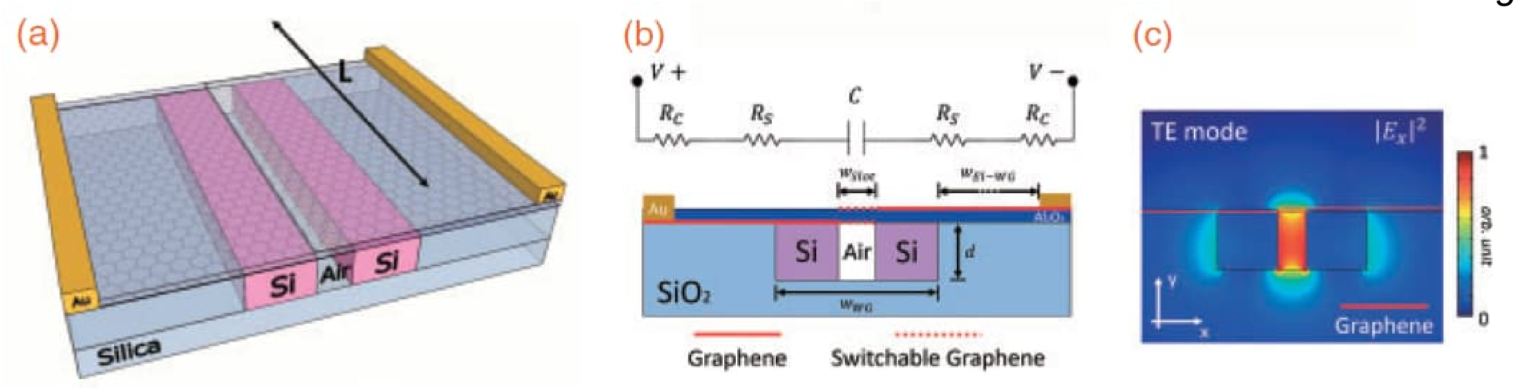

Surface conductivity of graphene sheet

Graphene *sheet conductivity* is usually expressed in the form of a Kubo formula*

$$\sigma_s(\omega,\mu_c,\tau,T) = -\frac{ie^2}{\pi\hbar^2}\left[\frac{1}{(\omega+i\tau^{-1})}\int_0^\infty E\left(\frac{\partial f(E)}{\partial E}-\frac{\partial f(-E)}{\partial E}\right)dE + (\omega+i\tau^{-1})\int_0^\infty \frac{f(E)-f(-E)}{(\omega+i\tau^{-1})^2-4(E/\hbar)^2}dE\right],$$

where $\omega = 2\pi c/\lambda$ … circular frequency of light

$\mu_c \approx v_F\sqrt{\pi(C_e/e)|V-V_D|}$ … chemical potential

$C_e = \varepsilon_0\varepsilon_d/d$ …capacity of electrodes per unit area

$v_F \approx 10^6$ m/s …Fermi velocity

$\tau \approx 0.01-1$ ps … time constant

$T \approx 300$ K … absolute temperature

$f(E) = \left\{\exp\left[(E-\mu_c)/k_BT\right]+1\right\}^{-1}$

. . . Fermi-Dirac distribution function,

V . . . voltage applied to the electrodes ("electrical doping" of graphene), and

V_D . . . voltage offset by graphene natural doping

We will use the following *approximate* closed-form formula** in our further considerations:

$$\boxed{\sigma_s(\omega,E_F,\tau,T) \approx \frac{e^2E_F}{\pi\hbar^2}\frac{i}{i/\tau+\omega} + \frac{e^2}{4\hbar}\left\{\frac{1}{2}\left[\tanh\left(\frac{\hbar\omega+2E_F}{4k_BT}\right)+\tanh\left(\frac{\hbar\omega-2E_F}{4k_BT}\right)\right]-\frac{i}{2\pi}\ln\left[\frac{(\hbar\omega+2E_F)^2}{(\hbar\omega-2E_F)^2+(2k_BT)^2}\right]\right\}}$$

where $E_F \approx \mu_c$ is the energy of Fermi level.

*T. Stauber et al., Phys. Rev. B, Vol. 78, 085432, 2008.

**Y.-C. Chang et al., Appl. Phys. Lett. Vol. 104, No. 26, 261909, 2014.

Spectral dependence of the surface conductivity

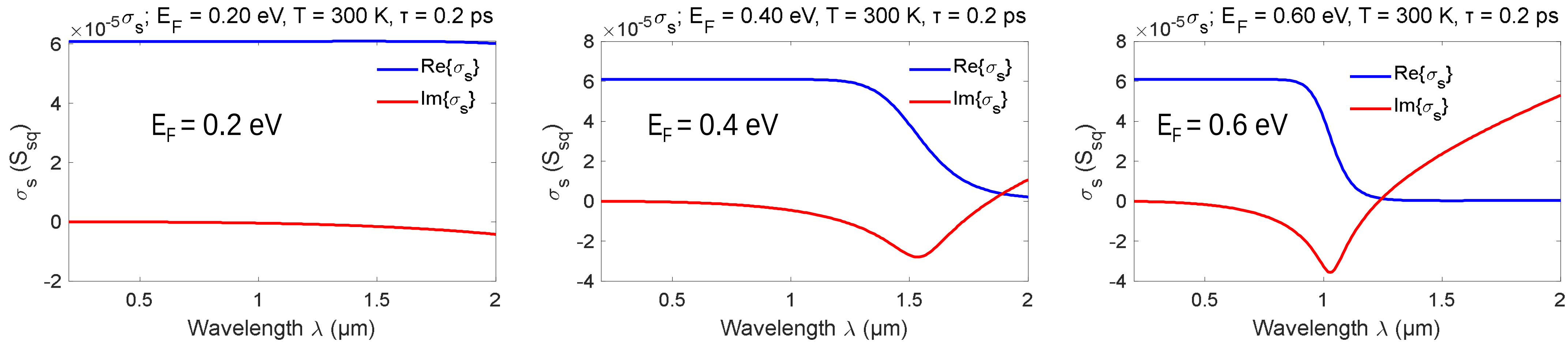

"Interesting region" for wavelength band around 1.55 μm takes place for E_F ~ 0.4 eV, for which $\hbar\omega \approx 2E_F$.

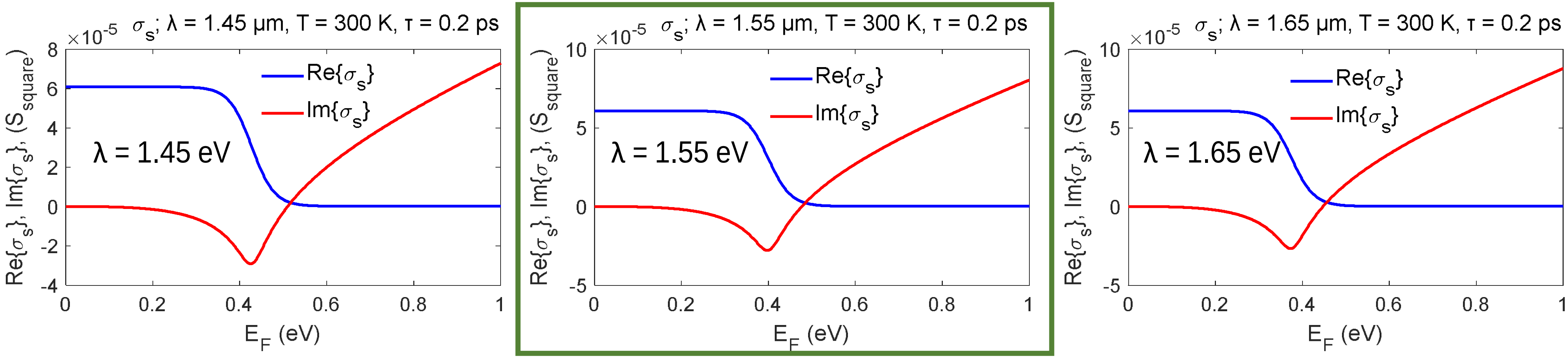

Graphene sheet as a “boundary condition” between $\boldsymbol{\varepsilon}_s$ and $\boldsymbol{\varepsilon}_a$

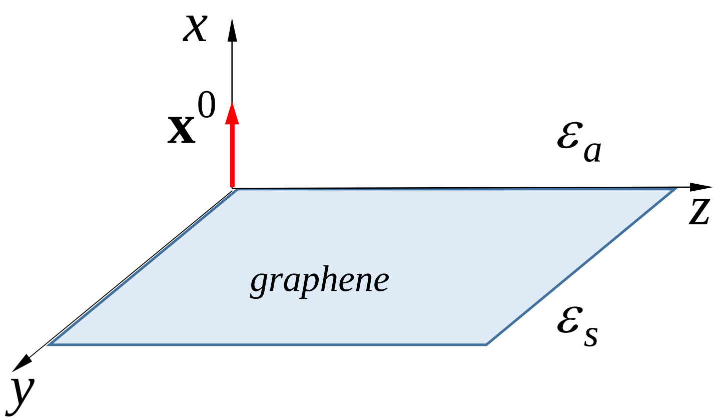

Tangential component of $\mathbf{E}$ is apparently

$$-\mathbf{x}^0\times\left(\mathbf{x}^0\times\mathbf{E}\right)=\mathbf{E}-\mathbf{x}^0(\mathbf{x}^0\cdot\mathbf{E})=$$

$$=\left(\mathbf{I}-\mathbf{x}^0\mathbf{x}^0\right)\cdot\mathbf{E}=\overline{\mathbf{P}}_x\cdot\mathbf{E}$$

Here, $\overline{\mathbf{P}}_x=\overline{\mathbf{I}}-\mathbf{x}^0\mathbf{x}^0$ is a (dyadic) projector to the plane perpendicular to $\mathbf{x}^0$,

$$\overline{\mathbf{P}}_x=\begin{pmatrix}0&0&0\\0&1&0\\0&0&1\end{pmatrix}.$$

Electric field continuity condition:

$$\boxed{\mathbf{x}^0\times\left(\mathbf{E}_s-\mathbf{E}_a\right)=\mathbf{0},}\qquad \Rightarrow \qquad \mathbf{x}^0\times\mathbf{E}_s=\mathbf{x}^0\times\mathbf{E}_a,$$

$$\left(\mathbf{I}-\mathbf{x}^0\mathbf{x}^0\right)\cdot\mathbf{E}_s=\left(\mathbf{I}-\mathbf{x}^0\mathbf{x}^0\right)\cdot\mathbf{E}_a,\ \text{or}\ \ \overline{\mathbf{P}}_x\cdot\mathbf{E}_s=\overline{\mathbf{P}}_x\cdot\mathbf{E}_a$$

Tangential component of electric field intensity induces surface current density $\mathbf{K}$:

$$\mathbf{K}=\sigma_s\overline{\mathbf{P}}_x\cdot\mathbf{E}_s=\sigma_s\overline{\mathbf{P}}_x\cdot\mathbf{E}_a.$$

Let us introduce the *sheet conductivity tensor*

$$\boxed{\overline{\boldsymbol{\sigma}}_s=\sigma\overline{\mathbf{P}}_x,\quad \overline{\boldsymbol{\sigma}}_s=\begin{pmatrix}0&0&0\\0&\sigma_s&0\\0&0&\sigma_s\end{pmatrix}.}$$

Magnetic field continuity condition sounds then

$$\mathbf{x}^0\times\left(\mathbf{H}_s-\mathbf{H}_a\right)=\mathbf{K},\ \ \text{or}$$

$$\boxed{\mathbf{x}^0\times\left(\mathbf{H}_s-\mathbf{H}_a\right)=\overline{\boldsymbol{\sigma}}_s\cdot\mathbf{E}_s=\overline{\boldsymbol{\sigma}}_s\cdot\mathbf{E}_a.}$$

"Volumetric" approach to graphene

Expanding the graphene sheet conductivity $\bar{\boldsymbol{\sigma}}_s$ into a layer of a finite thickness Δ, the "bulk" conductivity becomes

$$\bar{\boldsymbol{\sigma}}_b = \bar{\boldsymbol{\sigma}}_s / \Delta.$$

In accordance with Maxwell equation

$$\nabla \times \mathbf{H} = (-i\omega\varepsilon_0 \bar{\boldsymbol{\varepsilon}} + \bar{\boldsymbol{\sigma}}) \cdot \mathbf{E},$$

the complex (relative) permittivity is

$$\hat{\bar{\boldsymbol{\varepsilon}}} = \bar{\boldsymbol{\varepsilon}} + i\,\bar{\boldsymbol{\sigma}} / (\omega\varepsilon_0).$$

(we tacitly assume complex formalism for monochromatic waves with time dependence $\exp(-i\omega t)$).

For graphene we would get

$$\bar{\boldsymbol{\varepsilon}}_g = i\,\bar{\boldsymbol{\sigma}}_b / (\omega\varepsilon_0) = \frac{i\sigma_s}{\omega\varepsilon_0\Delta} \begin{pmatrix} 0 & 0 & 0 \\ 0 & 1 & 0 \\ 0 & 0 & 1 \end{pmatrix}.$$

However, most software requires calculation of $\bar{\boldsymbol{\varepsilon}}_g^{-1}$, but $\bar{\boldsymbol{\varepsilon}}_g$ is singular. To avoid problems, some "background permittivity" $\bar{\varepsilon}_b$ is usually added; the "volumetric permittivity" then reads

$$\boxed{\bar{\boldsymbol{\varepsilon}}_g = \bar{\boldsymbol{\varepsilon}}_b + i\,\bar{\boldsymbol{\sigma}}_s / (\omega\varepsilon_0\Delta).}$$

But *there is no clear guiding rule how to choose the value of the background permittivity*, and very different values can be found in literature.

Simple test structure: SOI planar waveguide with graphene

We decided to compare results of both approaches by numerical modelling of a simple structure for which *rigorous dispersion formulas does exist*: a planar waveguide.

Inspiration*:

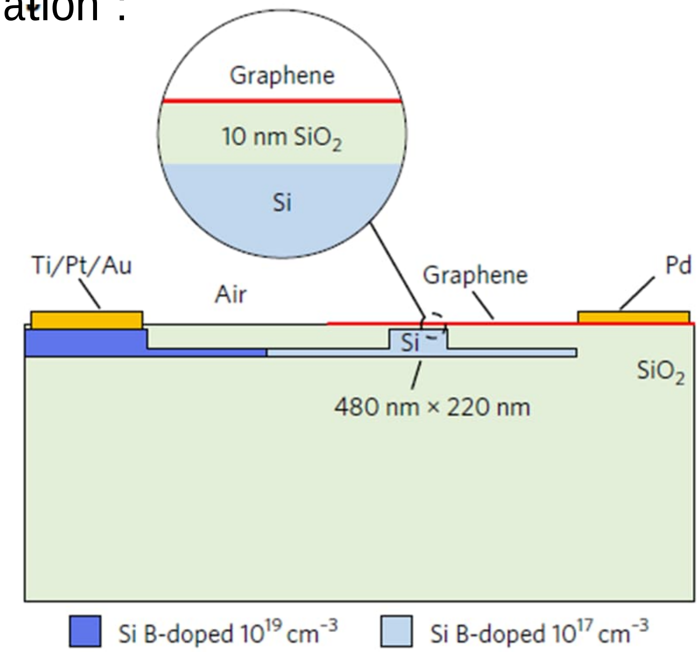

Simulation task:

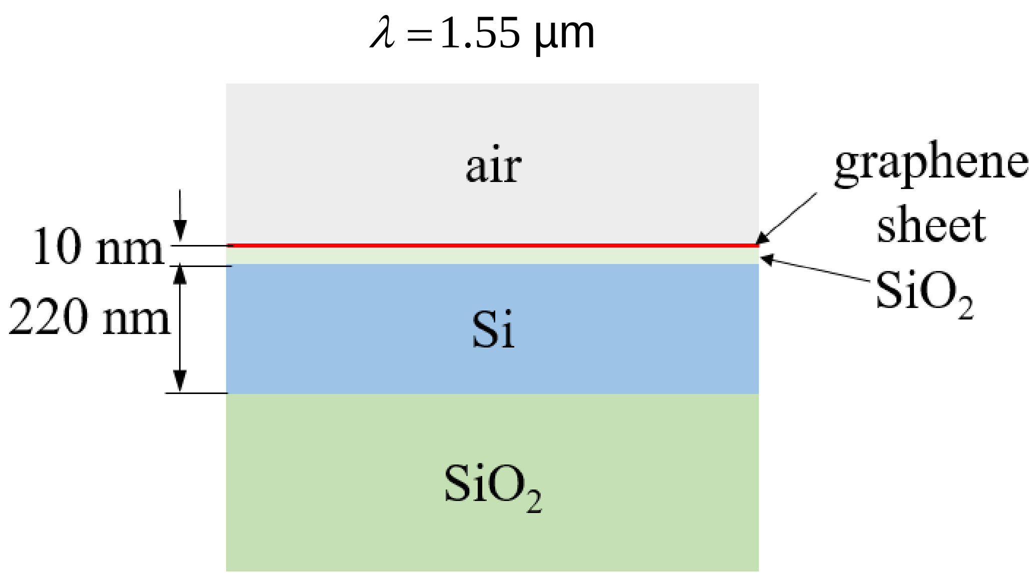

Task: Calculate the change of the effective refractive index of the guided mode due to the presence of graphene (in dependence of the position of the Fermi level).

*V. Sorianello *et al.*, *Nature Photonics,* vol. 120, no. 12, pp. 40-44, 2017.

Numerical comparison of b. c. and volumetric approaches

For both approaches, rigorous analytical dispersion formulas were numerically solved.

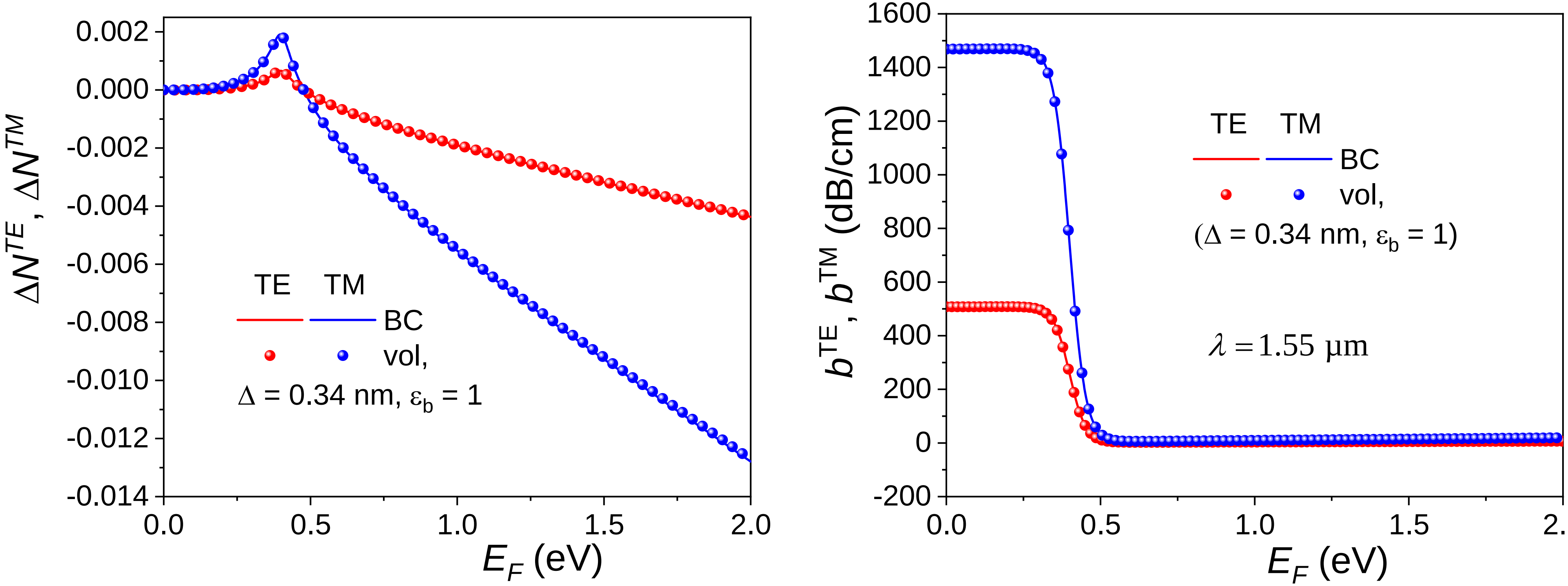

For very thin "artificial layer", Δ = 0.34 nm, and background permittivity 1, the results are practically identical.

(It is apparent that proper shifting the Fermi level results in an efficient phase or amplitude modulation…)

Influence of the “volumetric thickness” of the graphene

$\varepsilon_b = 1,$ thickness Δ = 0.34 to 10 nm

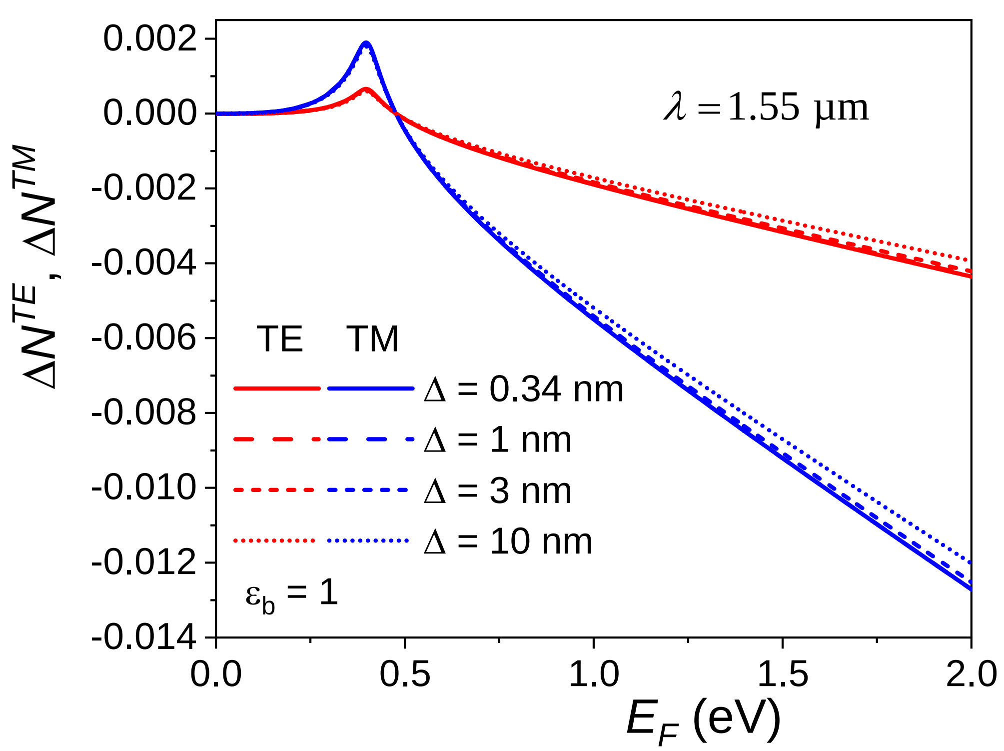

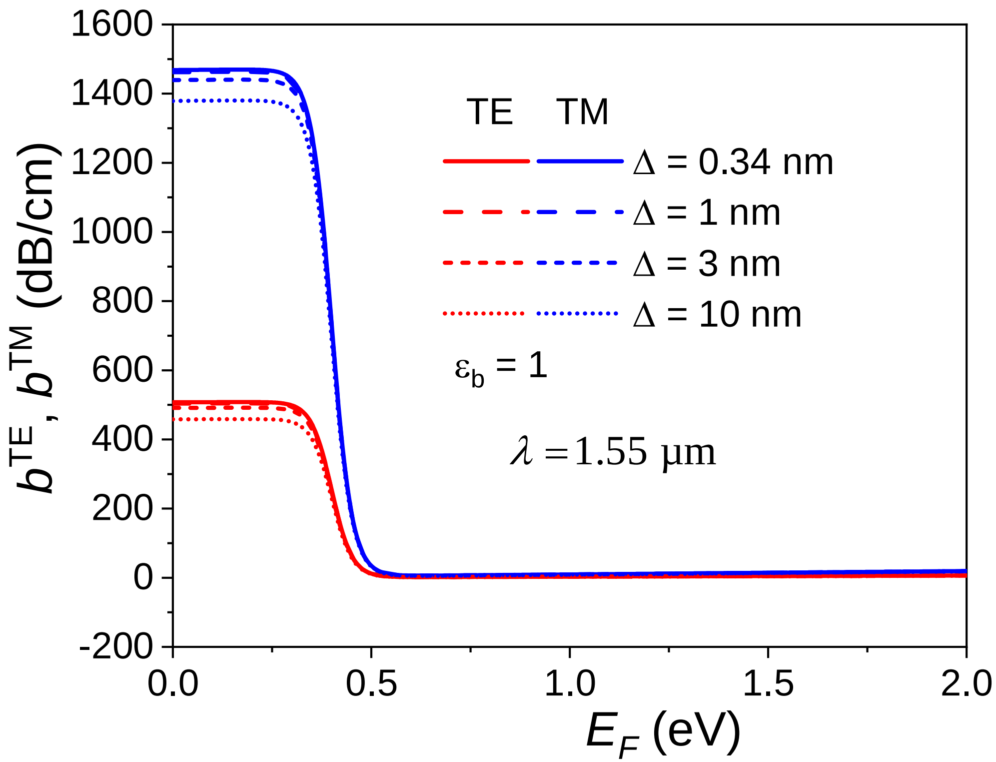

For $\varepsilon_b = 1$, the value of a “volumetric thickness” is not very critical.

Numerical comparison of different methods & approaches

$$\Delta\beta = \beta_g - \beta_0, \quad \Delta N = \mathrm{Re}\{\Delta\beta\}/k_0,$$

$$b = 2\times10^5 \log(e)\,\mathrm{Im}\{\beta\} \;\; [\mathrm{dB/cm;\ \mu m^{-1}}]$$

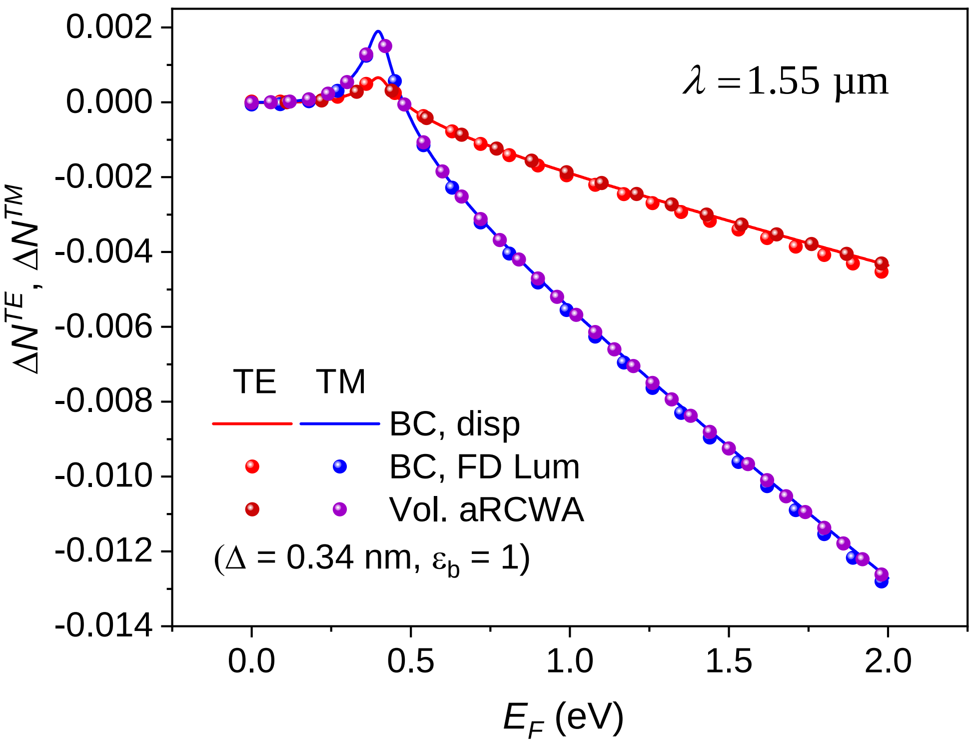

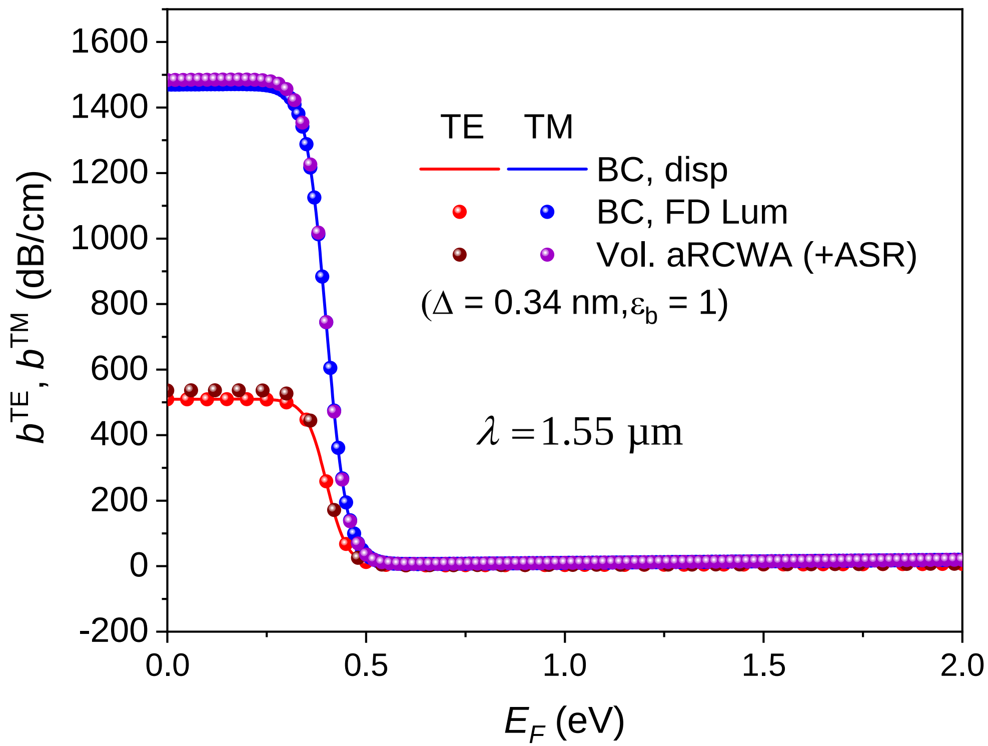

boundary condition approach: analytical disp. eq.
FDTD Lumerical
perturbation of Fresnel coeff.
FEM COMSOL, CST

'volumetric' approach: analytical disp. eq.
FMM aRCWA (+ ASR)
FEM COMSOL, CST

Similarity of $\boldsymbol{\varepsilon}_g$ and $\boldsymbol{\Delta} N_{eff}$

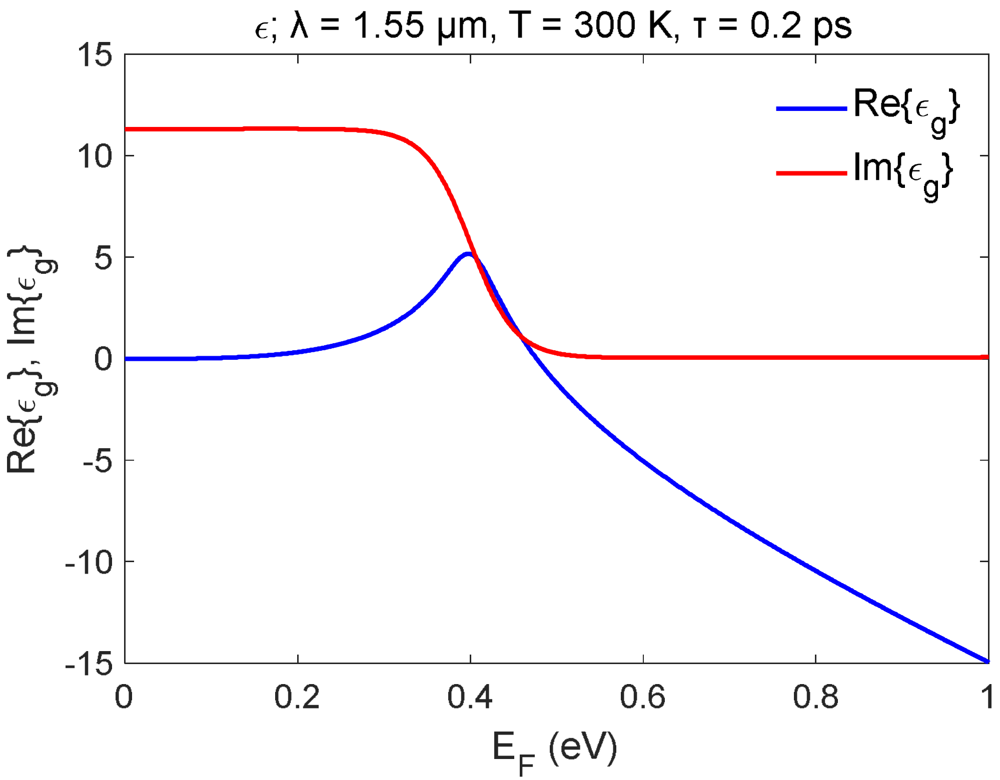

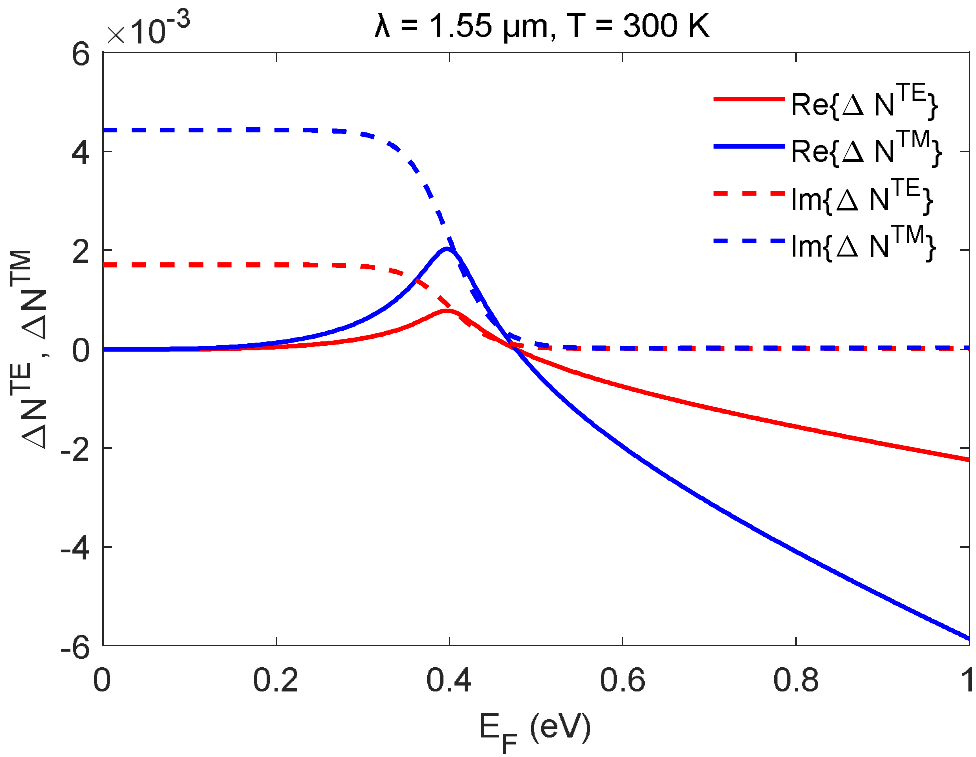

$$\varepsilon_g = i\frac{\sigma_s}{\omega\varepsilon_0}$$

$$\Delta N = N_{eff,gr} - N_{eff,no\,gr}$$

Similarity of these graphs indicates that *there might be a direct proportionality* between ε_g and ΔN

Perturbation approach

'Volumetric' graphene as a perturbation of the waveguide without graphene:

From the (complex) coupled mode theory*:

$$\Delta\beta \doteq \frac{\omega\varepsilon_0}{4}\iint_S \left[\mathbf{e}_\perp \cdot \Delta\varepsilon \cdot \mathbf{e}_\perp - \frac{\varepsilon^{(0)}}{\varepsilon^{(0)}+\Delta\varepsilon}\mathbf{e}_z \cdot \Delta\varepsilon \cdot \mathbf{e}_z\right] dS, \qquad \frac{1}{2}\iint_S \mathbf{e}_\perp(x,y)\times\mathbf{h}_\perp(x,y)\cdot d\mathbf{S} = 1,$$

From the reciprocity theorem it follows:

$$\Delta\beta = \frac{\omega\varepsilon_0}{4}\iint_S \left[\mathbf{e}_{1\perp} \cdot \Delta\varepsilon \cdot \mathbf{e}_{2\perp} - \mathbf{e}_z \cdot \Delta\varepsilon \cdot \mathbf{e}_z\right] dS,$$

$\mathbf{e}_1 \ldots$ (normalized) field without graphene,

$\mathbf{e}_2 \ldots$ (normalized) field with graphene

Supposing that either $\Delta\varepsilon$ or its volume (or both) are small, or $\mathbf{e}_1 \approx \mathbf{e}_2$,
for the lossless waveguide without graphene ($\mathbf{e}_\perp$ real, $\mathbf{e}_z$ imaginary), we obtain from both expressions

$$\boxed{\Delta\beta \approx \frac{\omega\varepsilon_0}{4}\iint_S \mathbf{e}\cdot\Delta\varepsilon\cdot\mathbf{e}^*\, dS}$$

*W.-P. Huang and J. Mu, *Opt. Express, vol. 17, pp. 19134-19152, 2009.*

Comparison of mode fields without and with graphene

Boundary condition approach, numerical solution of rigorous dispersion equation

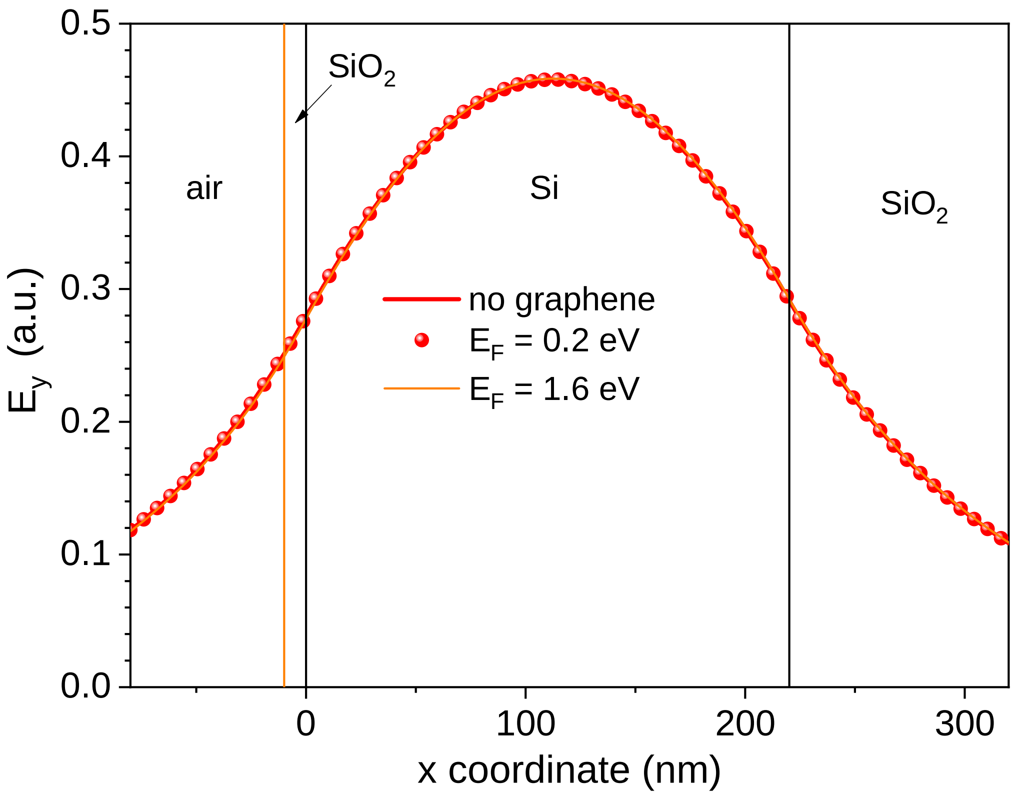

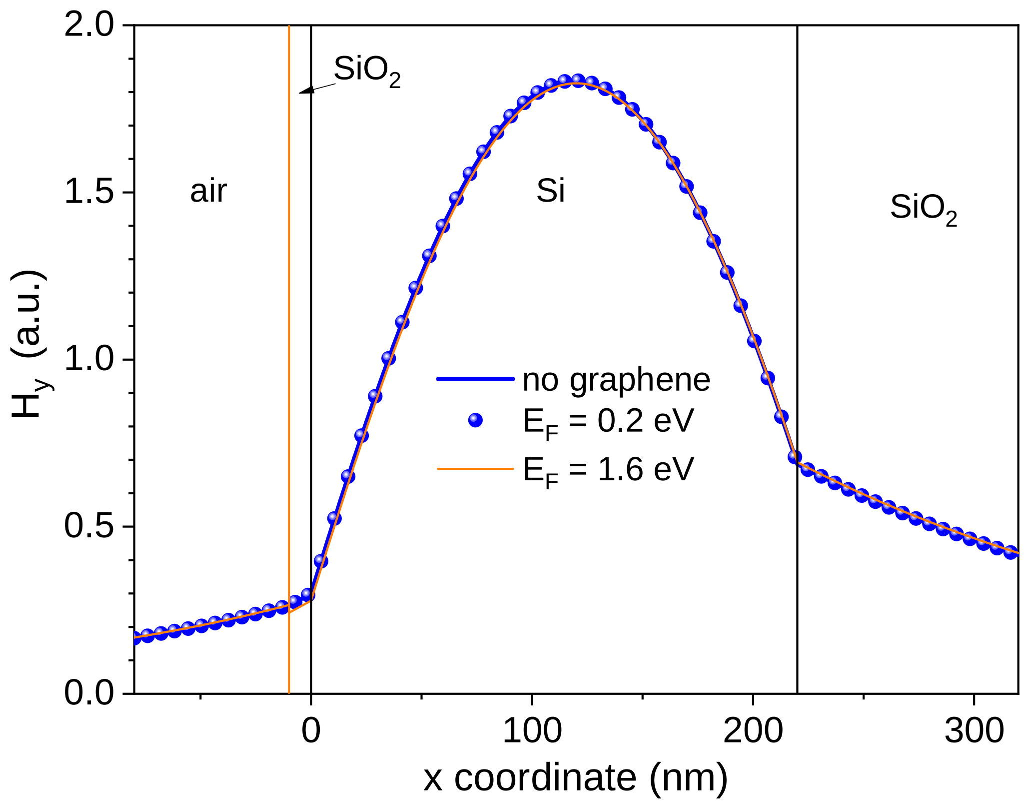

The mode field distribution is only very weakly influenced by the graphene layer (stronger for TM mode)

Generalized perturbation formula

This approach can be easily generalized to an arbitrarily shaped graphene layer (in the waveguide cross-section)*:

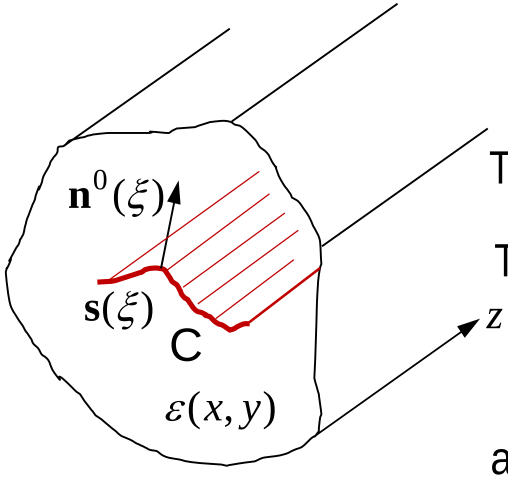

graphene layer is distributed along the curve C determined by the parametric function $\mathbf{s}(\xi)=\big(x(\xi),y(\xi),0\big)$ in the waveguide cross-section.

The normal vector to this surface is apparently $\mathbf{n}^0(\xi)=\dfrac{d\mathbf{s}(\xi)}{d\xi}\times\mathbf{z}^0$.

The permittivity perturbation due to the graphene sheet can then be written as

$$\Delta\bar{\varepsilon}=\frac{i\sigma_s}{\omega\varepsilon_0}\delta\big[\mathbf{r}_\perp-\mathbf{s}(\xi)\big]\bar{\mathbf{P}}(\xi),\quad \bar{\mathbf{P}}(\xi)=\bar{\mathbf{I}}-\mathbf{n}^{(0)}\mathbf{n}^{(0)},$$

and the perturbation of the propagation constant as

$$\boxed{\Delta\beta\approx\frac{i\sigma_s}{4}\int_C\mathbf{e}(\xi)\cdot\bar{\mathbf{P}}(\xi)\cdot\mathbf{e}^*(\xi)\,d\xi.}$$ Eventually, $$\boxed{\Delta\beta\approx\frac{i}{4}\int_C\sigma_s(\xi)\mathbf{e}(\xi)\cdot\bar{\mathbf{P}}(\xi)\cdot\mathbf{e}^*(\xi)\,d\xi}$$

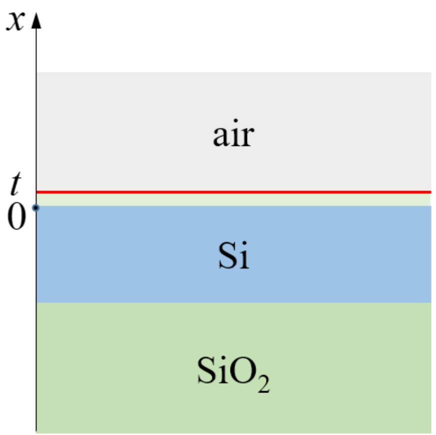

For *planar* waveguide, the perturbation of the propagation constant reduces to

$$\Delta\beta\approx\frac{i\sigma_s}{4}\mathbf{e}(t)\cdot\bar{\mathbf{P}}_x\cdot\mathbf{e}^*(t)=\frac{i\sigma_s}{4}\Big(\big|e_y(t)\big|^2+\big|e_z(t)\big|^2\Big).$$

* U. Ralević et al., J. Phys. D: Appl. Phys. 48, art. No. 355102, 2015

Comparison of perturbation and boundary condition approaches

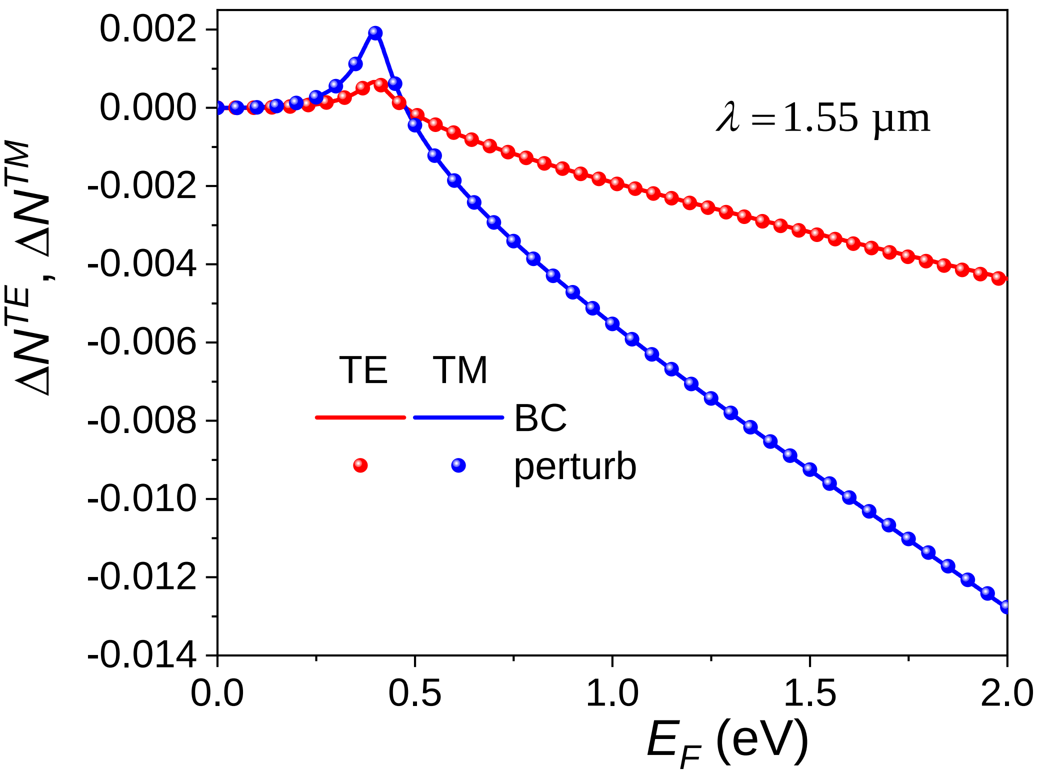

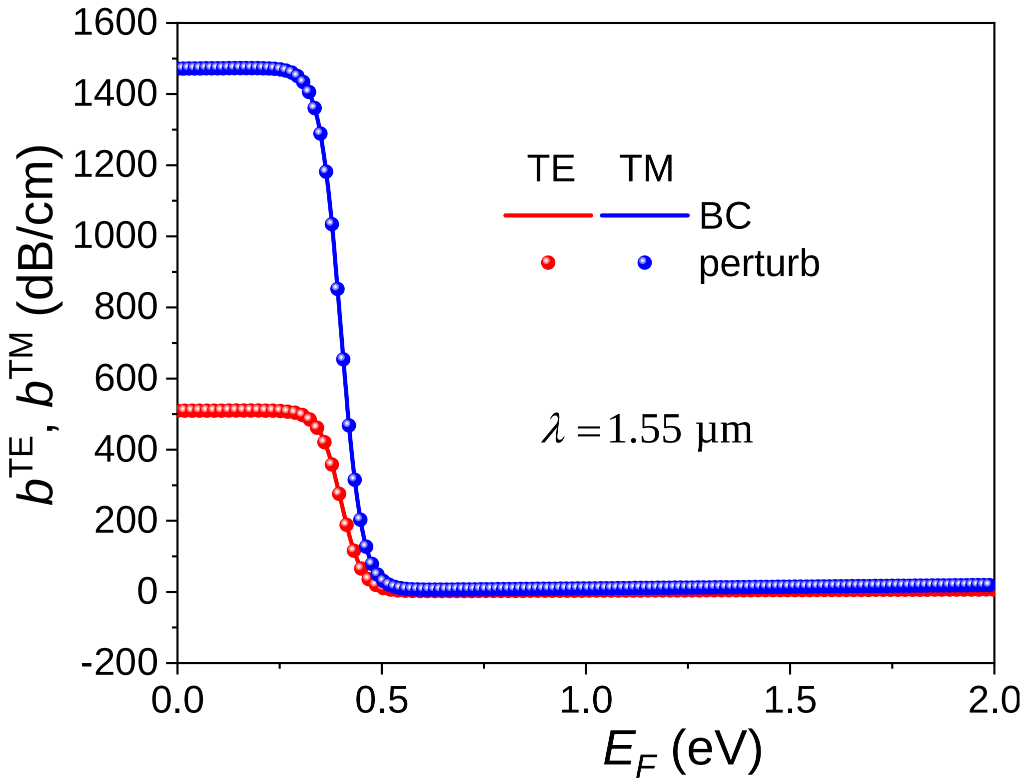

Perturbation method is probably the simplest and most versatile method for the design of waveguide devices containing graphene layers.

J. Čtyroký, J. Petráček, P. Kwiecien, I. Richter, and V. Kuzmiak, "Graphene on an optical waveguide: comparison of simulation approaches, Optical and Quantum Electronics, vol. 52, 149, 2020, doi: https://doi.org/10.1007/s11082-020-02265-0.

Surface plasmons on a graphene sheet

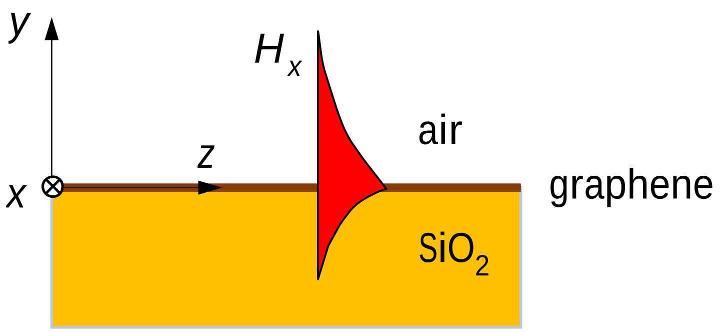

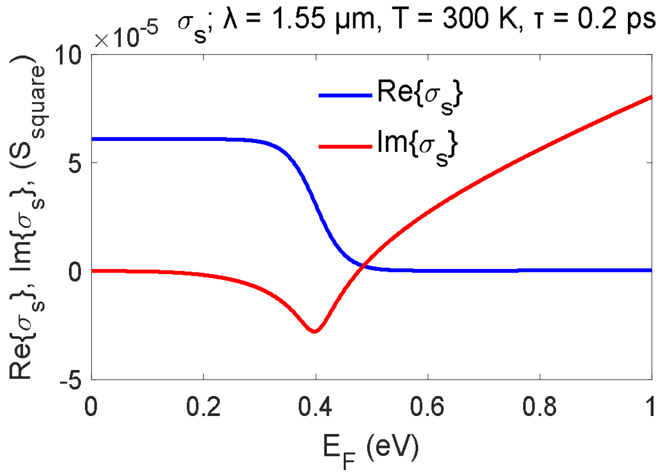

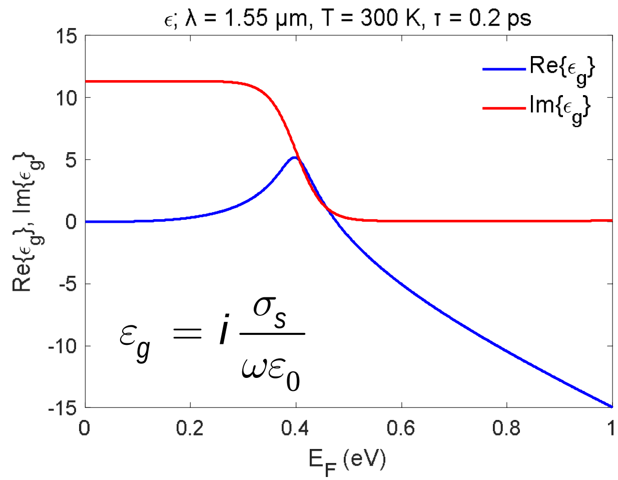

Expected TM surface plasmon field distribution:

$$(H_x, E_y, E_z) = (H_{x,1}, E_{y,1}, E_{z,1})\exp\left(ik_0 N_{sp} z - k_0 p_1 y\right),\ y > 0,$$

$$(H_x, E_y, E_z) = (H_{x,2} E_{y,2}, E_{z,2})\exp\left(ik_0 N_{sp} z + k_0 p_2 y\right),\ y < 0,$$

From Maxwell equations:

$$E_{y,1} = Z_0 \frac{N_{sp}}{\varepsilon_{air}} H_{x,1},\quad E_{y,2} = Z_0 \frac{N_{sp}}{\varepsilon_{SiO_2}} H_{x,2},\ Z_0 = \sqrt{\frac{\mu_0}{\varepsilon_0}},$$

$$E_{z,1} = -iZ_0 \frac{p_1}{\varepsilon_{air}} H_{x,1},\ E_{z,2} = iZ_0 \frac{p_2}{\varepsilon_{SiO_2}} H_{x,2}.$$

Field continuity conditions:

$$E_{z,2} = E_{z,1} = E_z,\ H_{x,2} - H_{x,1} = \sigma_s E_z.$$

Dispersion equation of a graphene surface plasmon:

$$\boxed{\frac{\varepsilon_{air}}{p_1} + \frac{\varepsilon_{SiO_2}}{p_2} = -iZ_0\sigma_s.}$$

The dispersion equation of a plasmon

on a metal/dielectric interface is $\dfrac{\varepsilon_d}{p_d} + \dfrac{\varepsilon_m}{p_m} = 0.$

Surface plasmons on a graphene sheet at **λ** = 200 µm

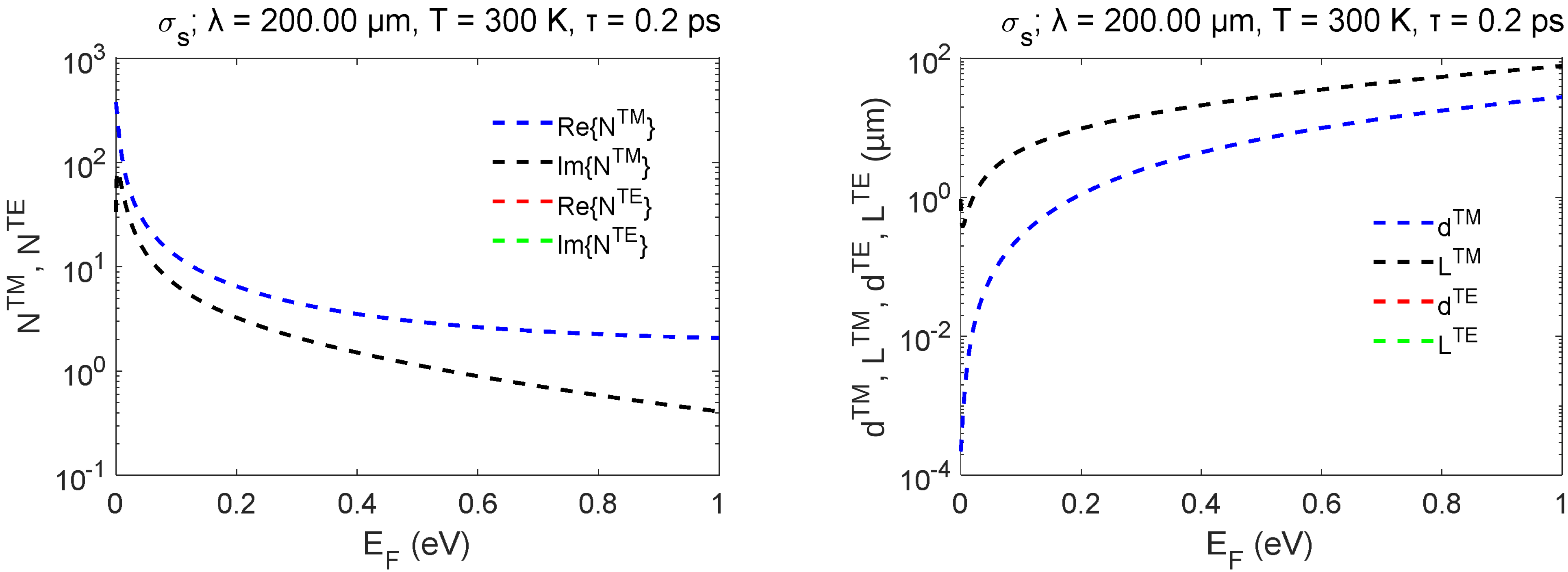

In THz spectral region ($\lambda = 200$ µm $\sim f = 1.5$ THz), the plasmons on the graphene sheet are somewhat similar to those on a metal/dielectric interface (the penetration depth ~ 1 µm, the propagation length ~ 10 µm).

Surface plasmons on a graphene sheet at λ = 1550 nm

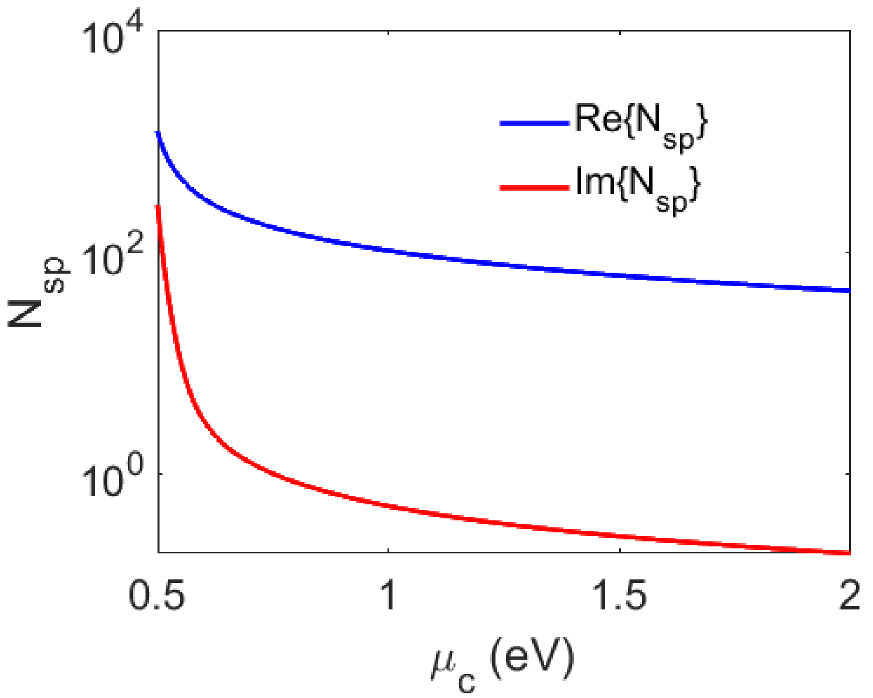

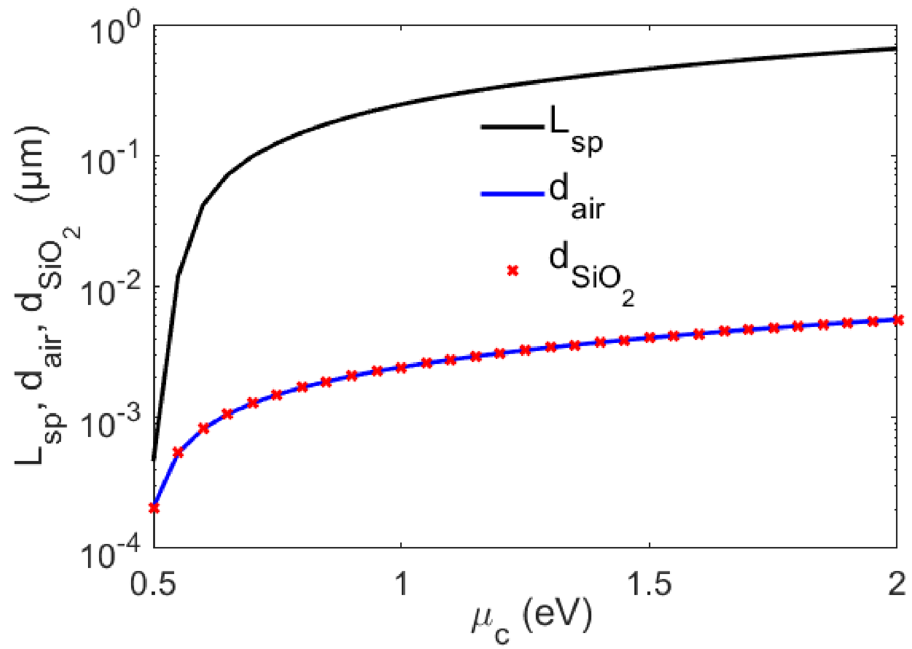

At $\lambda = 1550$ nm, the graphene surface plasmons are *extremely strongly localized,* with the penetration depth of the order of a few nm and the propagation length below 1 µm.

„Ribbon plasmons“

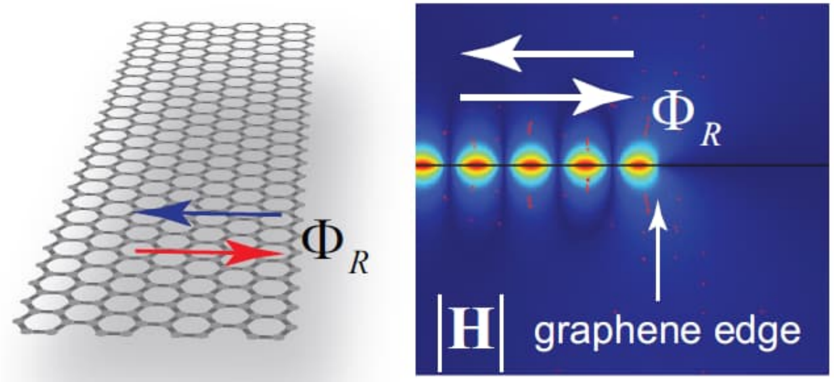

A.Y. Nikitin, T. Low, and L. Martin-Moreno, "Anomalous reflection phase of graphene plasmons and its influence on resonators,„ Physical Review B, vol. 90, no. 4, 041407, 2014

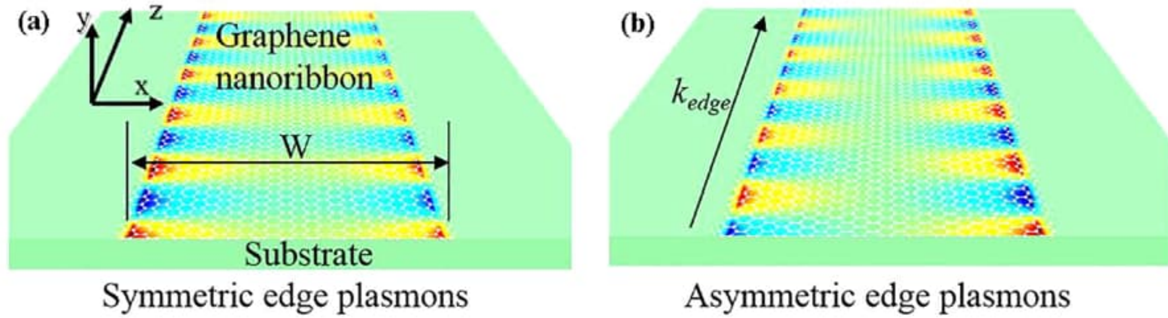

H. W. Hou, J. H. Teng, T. Palacios, and S. Chua, "Edge plasmons and cut-off behavior of graphene nano -ribbon waveguides," Opt. Commun., vol. 370, pp. 226-230, 2016.

Why are we interested in ribbon plasmons? Since the "canonic" electro-optic modulator using graphene looks as in the figure on the right.

The differences from the structures above: wavelength $\lambda \approx 1550$ nm, width $w \approx 500$ nm, graphene snadwichedd between SiO_2 and air.

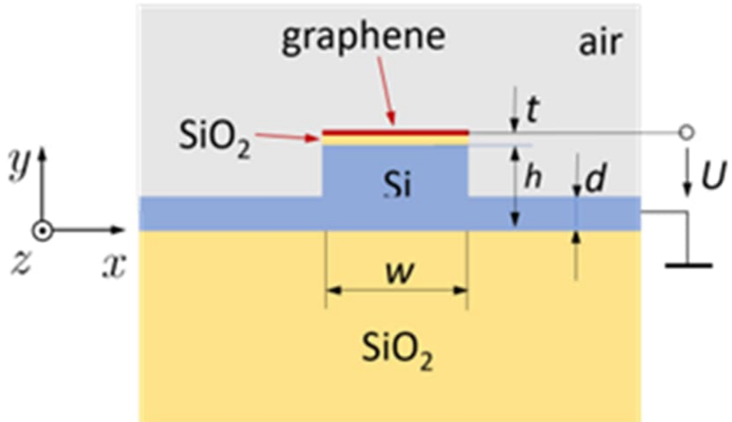

Effect of the coupling of the TE guided mode with graphene plasmons

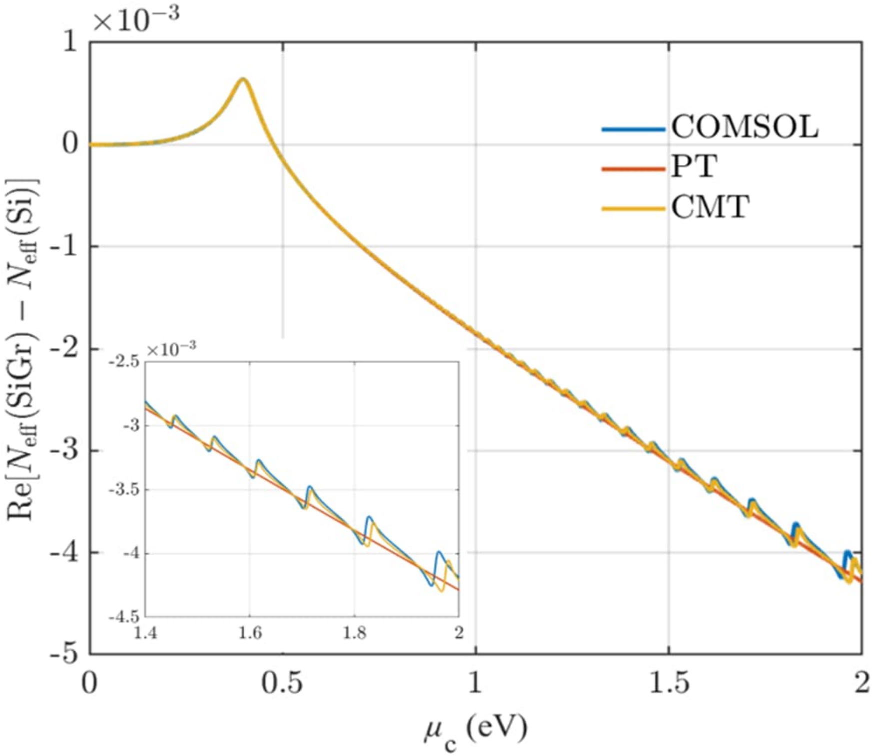

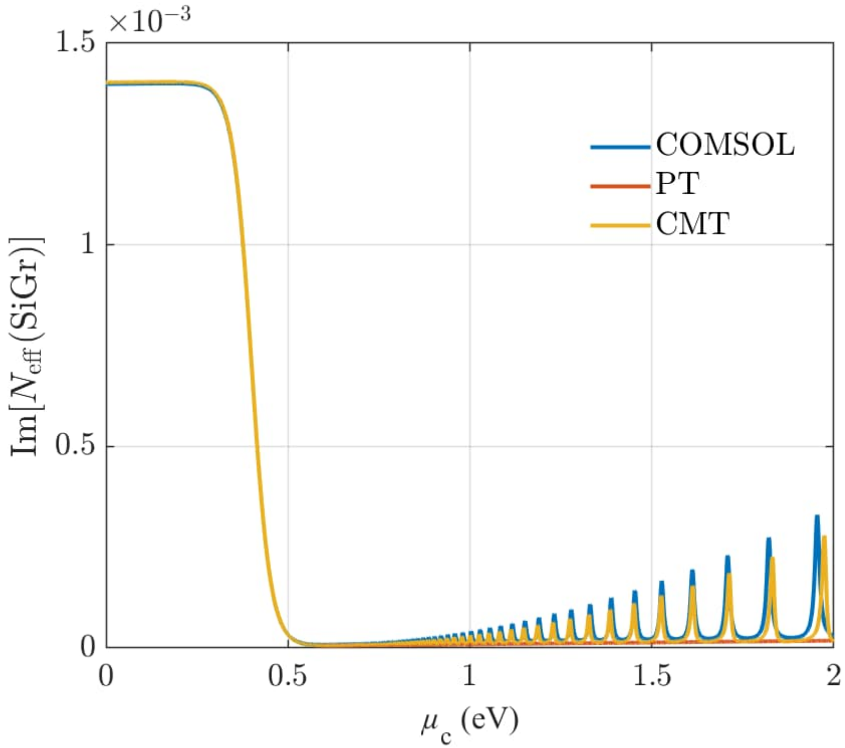

Coupling with graphene plasmon "ribbon" modes affects both the real and imaginary parts of the effective refractive index of the (quasi)TE guided mode, in dependence of the applied voltage. This effect can be both harmful and useful, depending on the concrete situation.

“Ribbon plasmons” on the graphene stripe

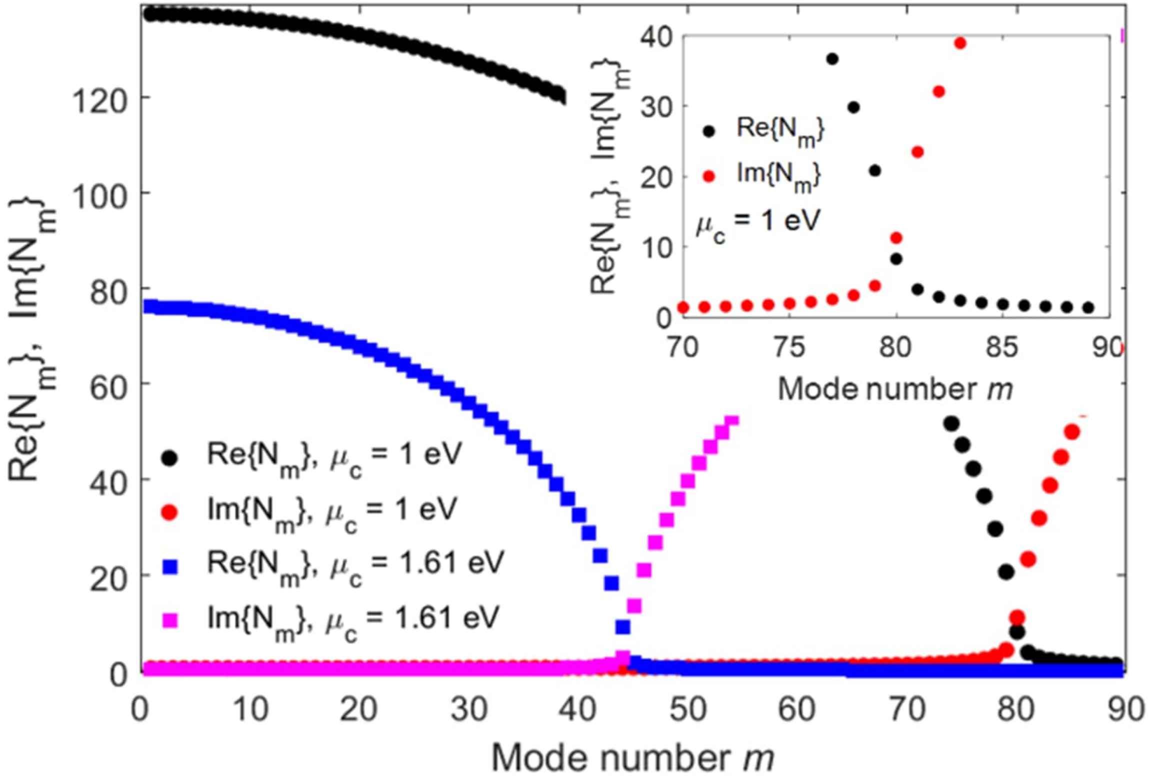

Due to the very high effective refractive index of the surface plasmon on the graphene stripe (Re{N^{sp}} is of the order of 10 to 100), there is a very large number of "ribbon plasmons" on the stripe.

Those with propagation constant (along z) close to N_{eff} of the silicon nanowire can couple with the guided mode and affect both the real and imaginary parts of its N_{eff}.

To keep the analysis as simple as possible, we approximated the (complicated) reflections at the edge of the graphene stripe by the refletion from a perfectly magnetically conducting "hard wall".

E_x field distribution of the TE mode of the silicon nanowire coupled with the “ribbon plasmon” on the graphene stripe

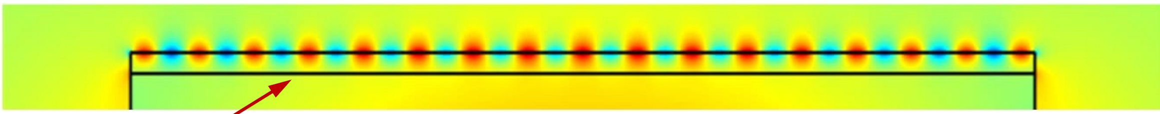

Zoomed field distribution of “ribbon plasmons” calculated by using COMSOL

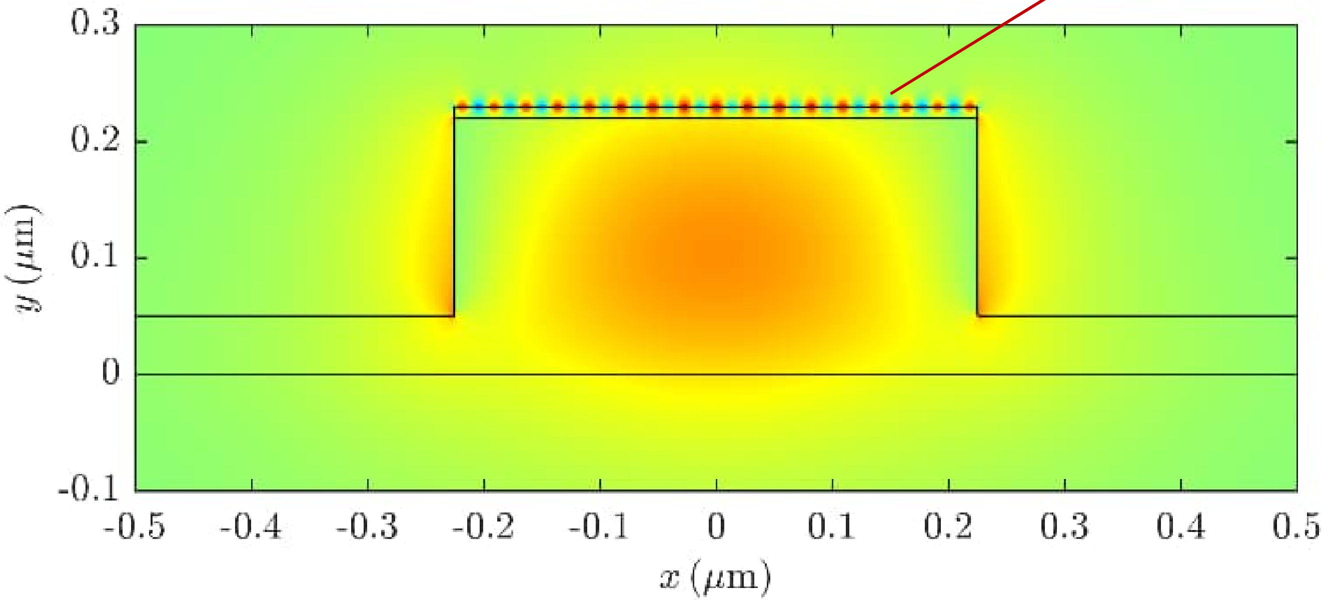

J. Čtyroký, J. Petráček, V. Kuzmiak, P. Kwiecien, and I. Richter, "Silicon waveguides with graphene: coupling of waveguide mode to surface plasmons," Journal of Optics, vol. 22, no. 9, 095801, 2020, doi: 10.1088/2040-8986/aba965.

The End of graphene-decorated waveguides;

Bound “states” (modes) in the continuum (BICs)

in integrated photonics

Bound states in the continuum (BICs)

Originally, a theoretical question of quantum physics about the existence of a discrete bound state with energy within the energy band of continuous states. Solved by J. von Neumann and E.P. Wigner in J. von Neumann, E. P. Wigner: Über merkwürdige diskrete Eigenwerte. *Physikalische Zeitschrift*, 1929;30:465-7.

Later, renowned interest in condensed matter physics and recently also in photonics.
A number of various photonic structures have been identified which support BICs;
they are typically resonant structures (gratings and photonic crystals) which support the existence of a bound mode with (theoretically) infinite Q-factor within a continuous spectrum of radiation modes, bound (lossless) waveguide modes with effective refractive indices lying within a continuum of radiation modes, and some other structures. Any coupling of the bound modes with the continuum introduces radiation loss; such modes with small losses are called *quasi-BICs* (q-BICs); in terms of traditional waveguide terminology, the q-BICs are, in fact, (low-loss) *leaky modes*. In the next slides we present a few examples of waveguide BICs and q-BICs.

“Classical” integrated optic waveguides (so far unidentified as BICs): Ti:$LiNbO_3$ and APE $LiNbO_3$ waveguides

X-cut Ti:$LiNbO_3$ planar waveguides

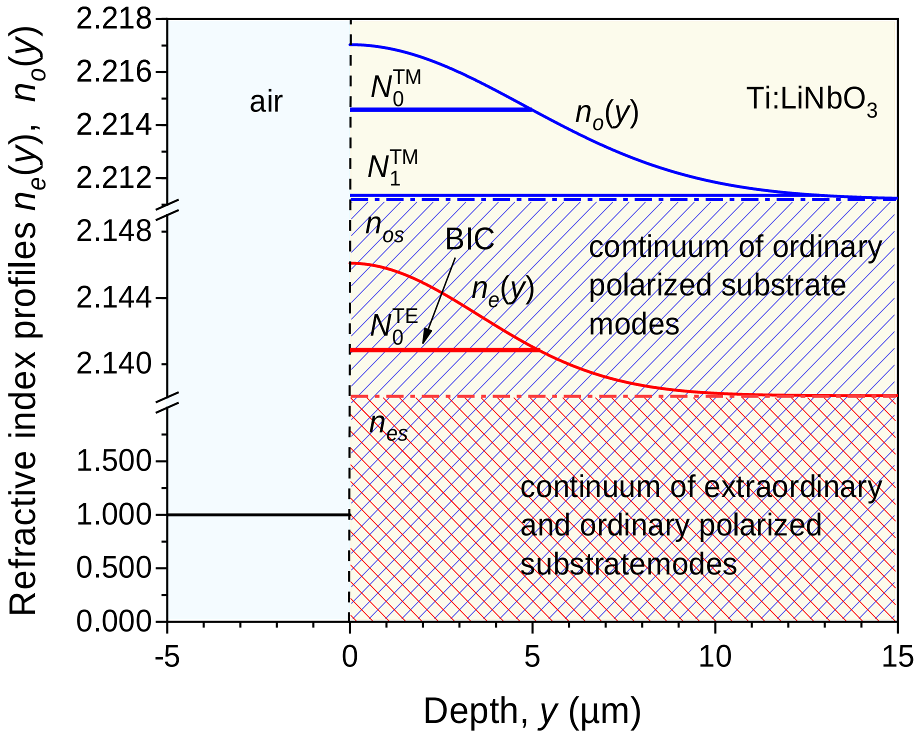

X-cut APE $LiNbO_3$ planar waveguides

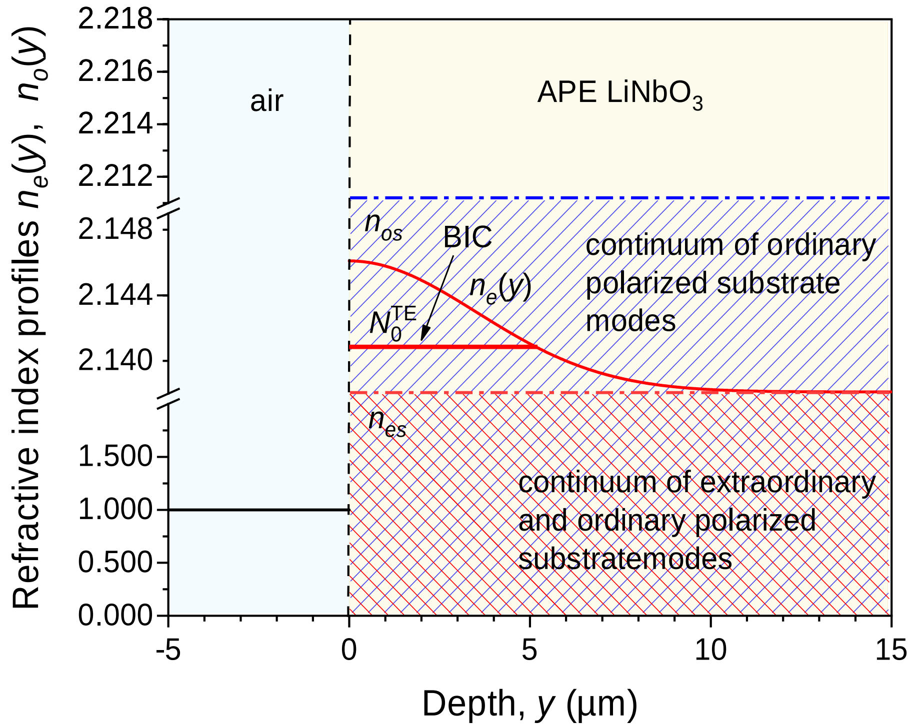

TE modes of planar waveguides – *polarization-protected* true (lossless) BICs due to $LiNbO_3$ birefringence

X-cut Y-propagating *channel* Ti:$LiNbO_3$ waveguides:
q-TE modes are (weakly) coupled to ordinary polarization -> loss -> qBICs

Permittivity in coordinates (x, y, z):
(z-propagation)

$$\begin{pmatrix} n_e^2 & 0 & 0 \\ 0 & n_o^2 & 0 \\ 0 & 0 & n_o^2 \end{pmatrix}$$

$$n_0 - n_e = 0.07316 > \Delta n_e = 0.008$$

Channel depth: 5 µm, width *w* varies from 5 to 10 µm.

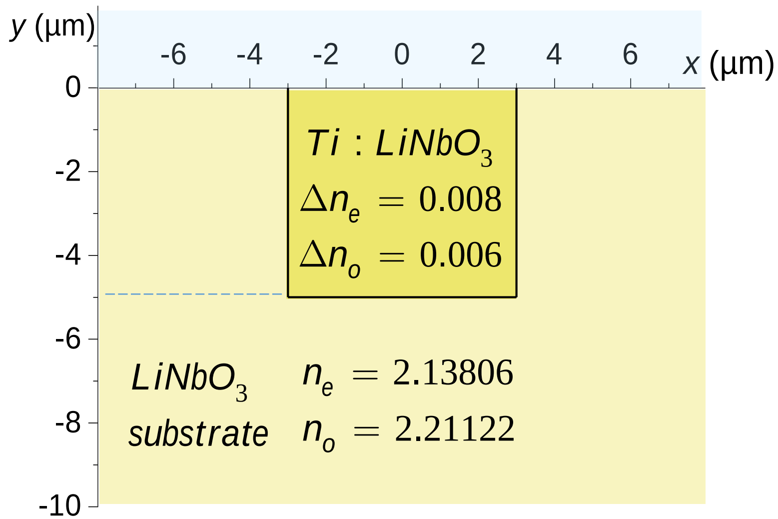

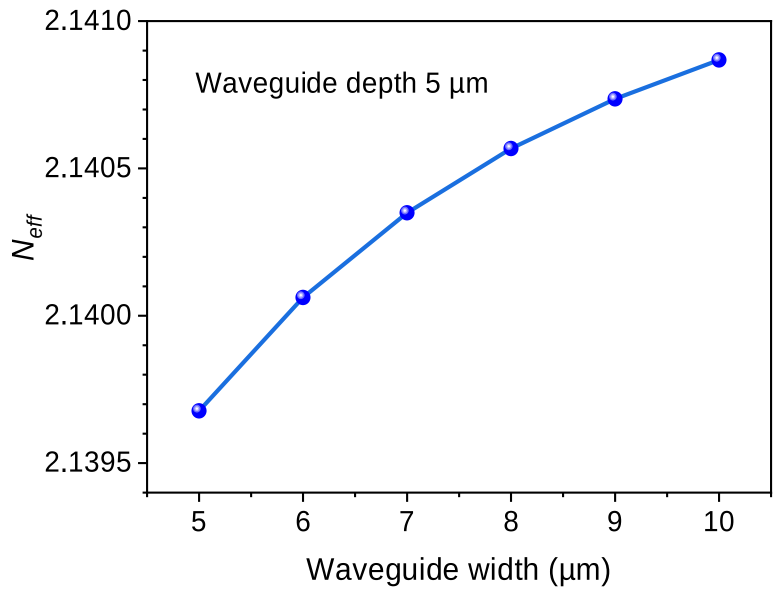

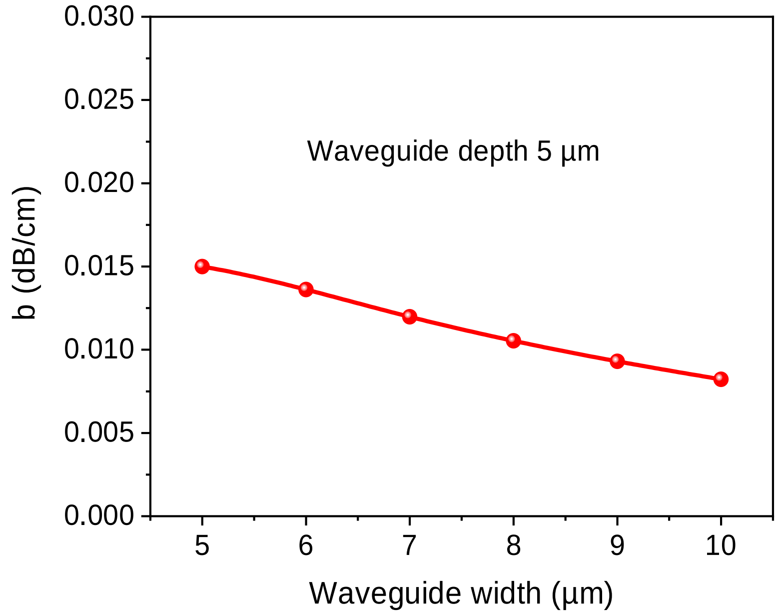

Off-axis propagation introduces loss due to coupling from guided extraordinary to unguided ordinary polarization. A few tens degrees off-axis propagation -> qBICS

x,*y*,*z* ...*crystallographic*
axes of $LiNbO_3$

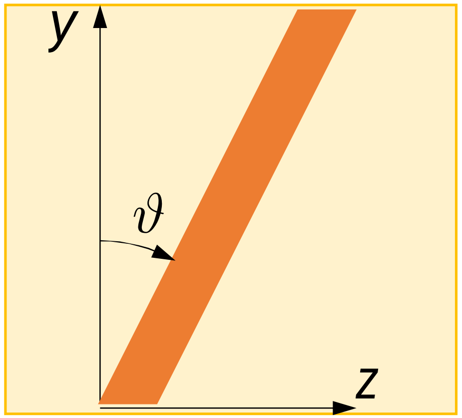

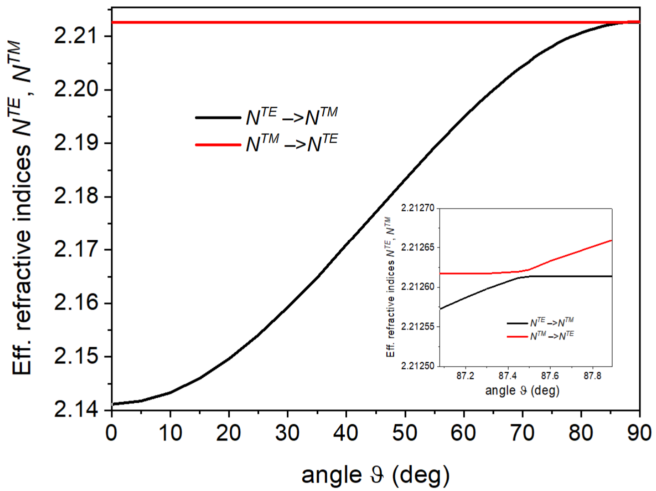

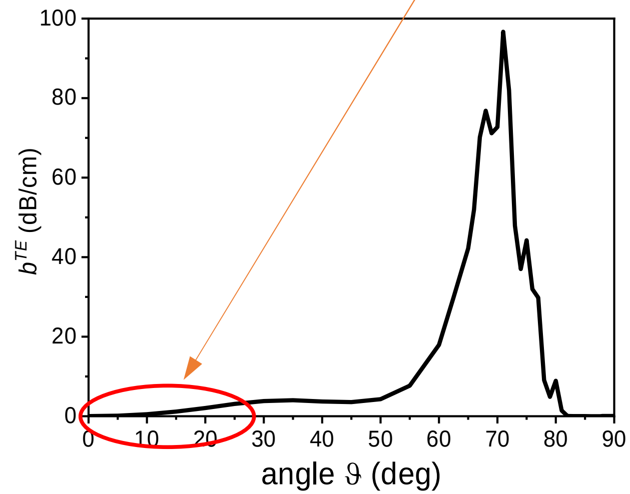

Angular dependence of the effective index and loss of the quasi-TE_{00} mode of the channel Ti:$LiNbO_3$ waveguide

(q-)BICs using LNOI waveguide platform

Polymer-loaded LNOI waveguide

LN permittivity in *waveguide* coordinates (x, y, z):
(z-propagation)

$$\begin{pmatrix} n_o^2 & 0 & 0 \\ 0 & n_e^2 & 0 \\ 0 & 0 & n_o^2 \end{pmatrix}$$

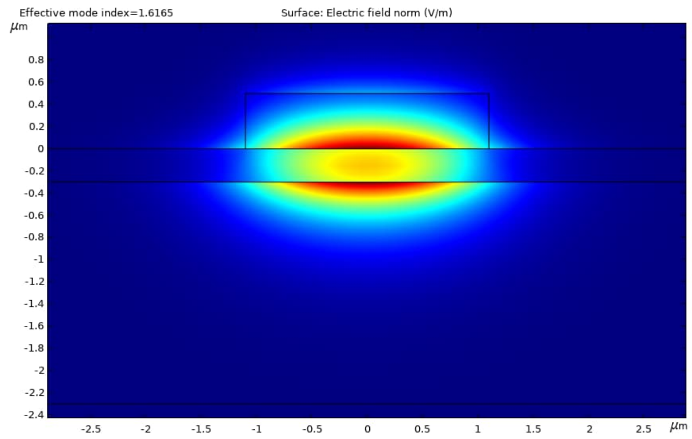

$$d_{LN} = 300\text{ nm},$$

$$h_{poly} = 500\text{ nm}, \quad n_{poly} = 1.5429$$

$$w_{poly} = 0 - 5\ \mu\text{m},\ SiO_2\text{ substrate, air cladding}$$

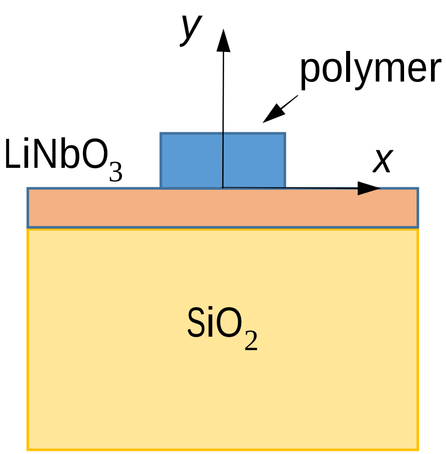

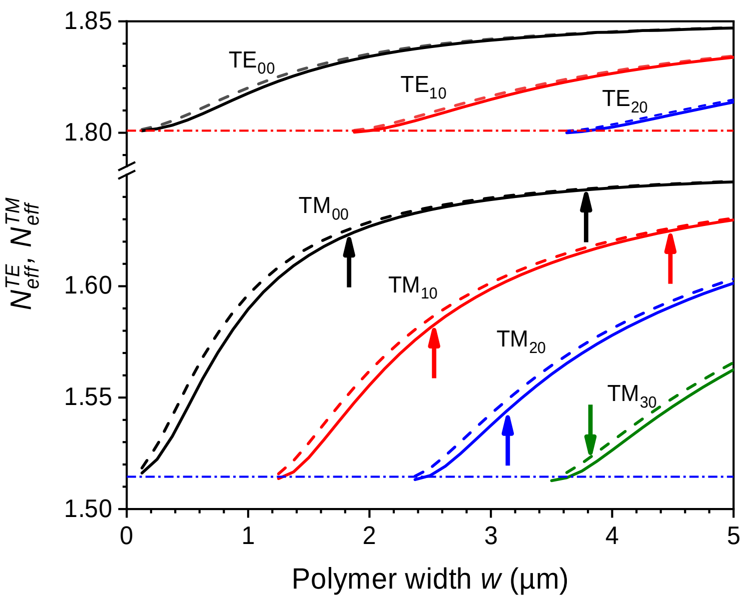

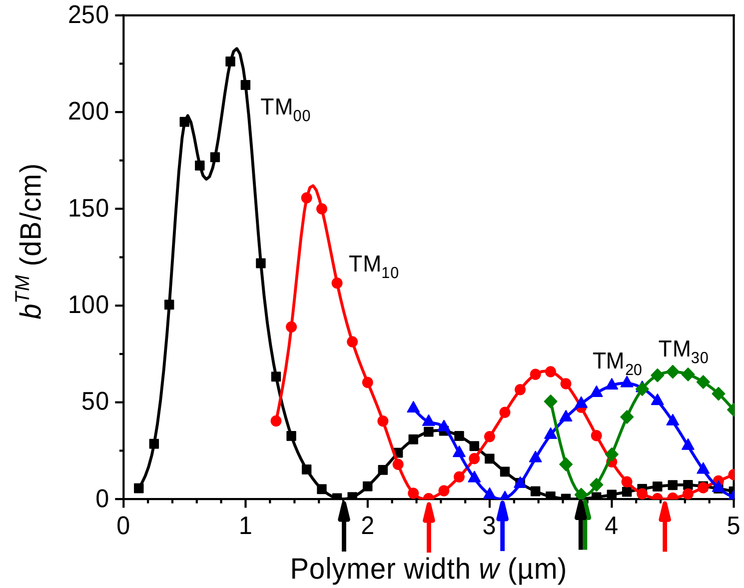

Proposed application of (q-)BIC waveguides for the design of integrated photonic devices

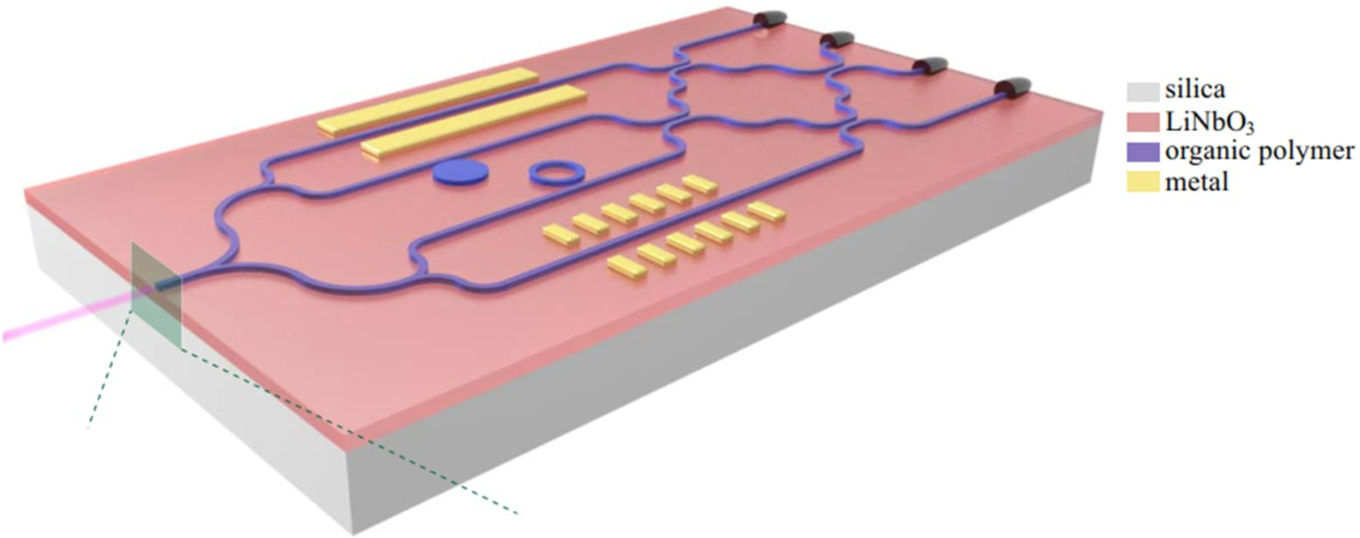

Z.J. Yu et al.: Photonic integrated circuits with bound states in the continuum. Optica. 2019;6(10):1342-8.

Operation of such structures has been experimentally verified.
Problems *not discussed* in the paper: *multimode* regime (existence of TM_{10} mode);
rather low mode overlap with $LiNbO_3$ crystal -> limited efficiency of electro-optic modulation;
incorrect analysis of electro-optic interaction,...

Shallow rib q-BIC LNOI waveguides

LN permittivity in coordinates (x, y, z): $\begin{pmatrix} n_o^2 & 0 & 0 \\ 0 & n_e^2 & 0 \\ 0 & 0 & n_o^2 \end{pmatrix}$
(z-propagation)

$d_{LN} = 250$ nm,
$h_{rib} = 150$ nm, $n_{poly} = 1.5429$
$w_{rib} = 0 - 3$ µm, SiO_2 substrate, air cladding

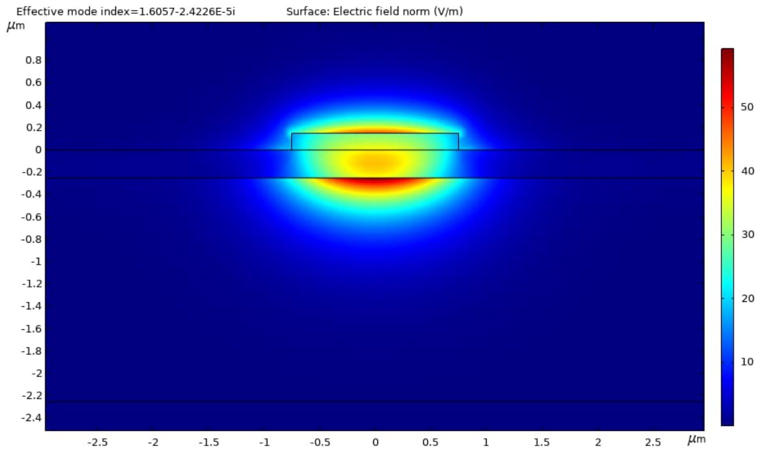

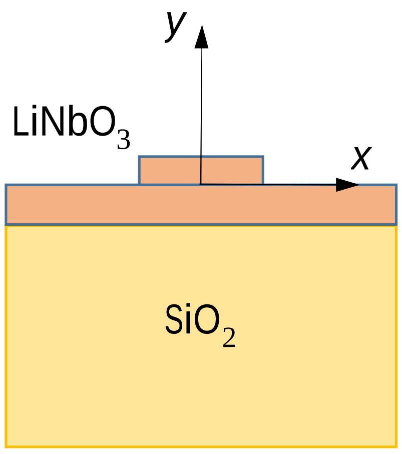

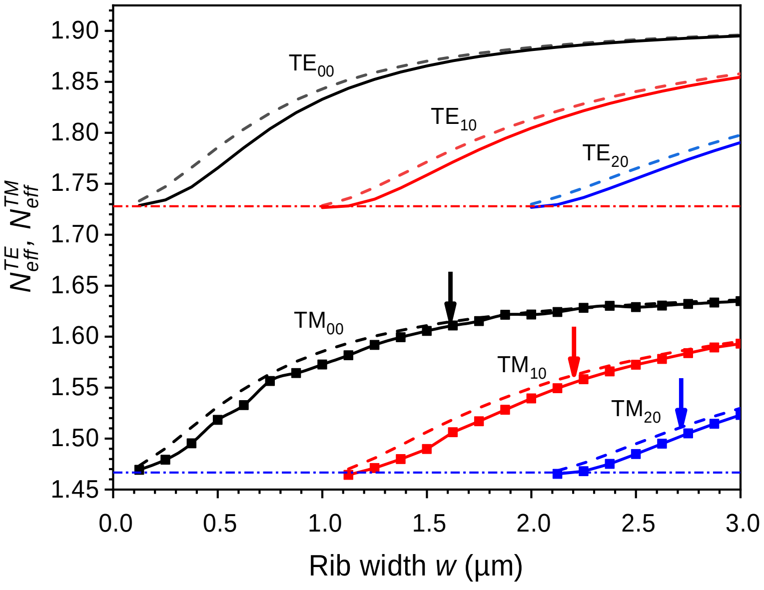

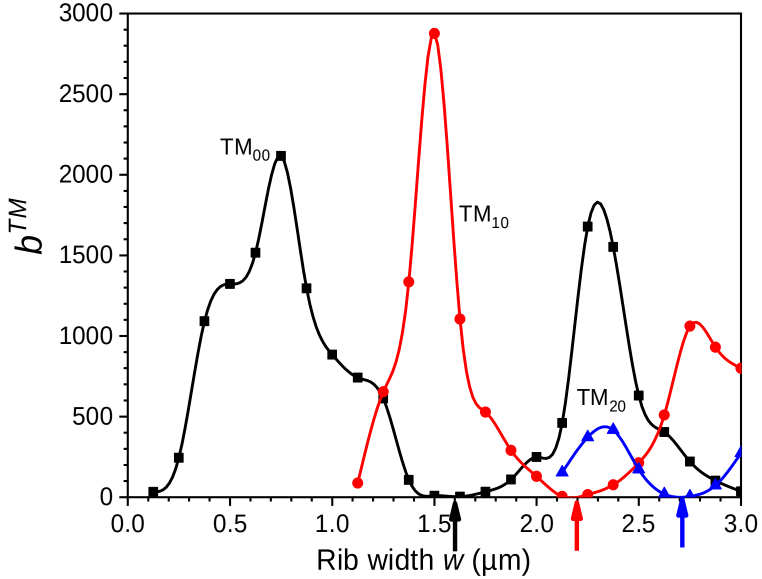

Uneasy fabrication; multimode operation, higher loss -> unprobable application

Shallow rib q-BIC SOI waveguides

$d_{Si} = 150$ nm,
$h_{rib} = 150$ nm,
$w_{rib} = 0 - 1.5$ µm, SiO_2 substrate, SiO_2 cladding

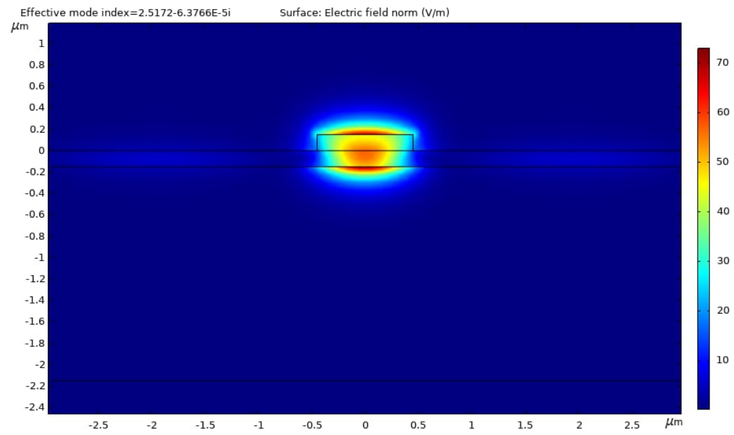

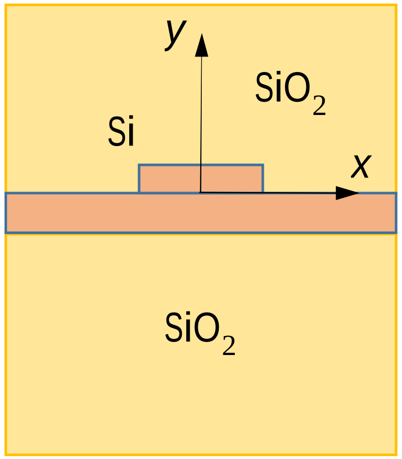

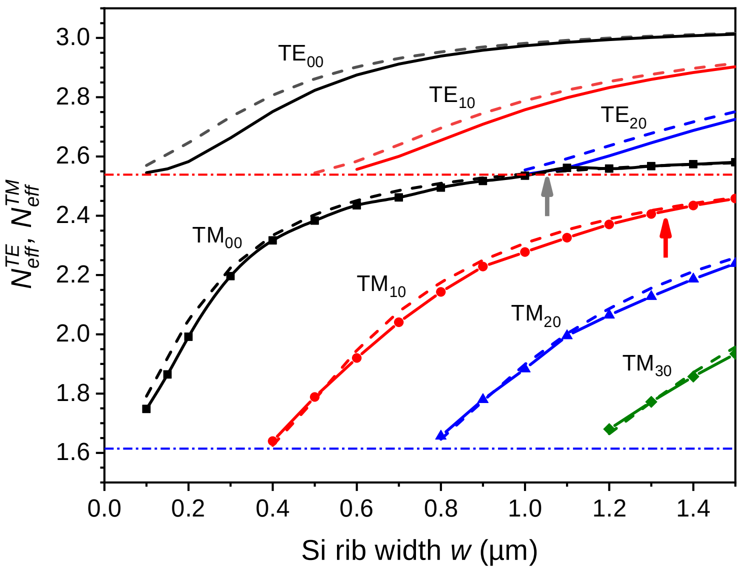

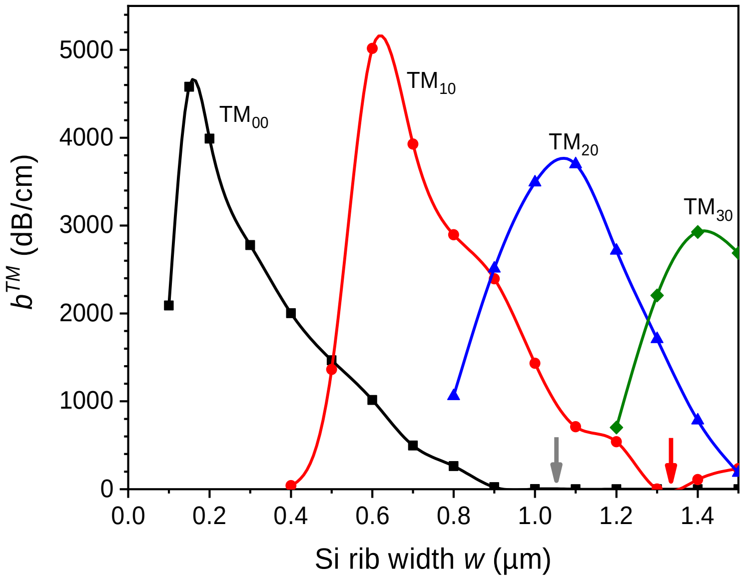

Similar difficulties as with shallow rib LNOI waveguides

Deep APE LNOI waveguides – lossless BICs!

LN permittivity in coordinates (x, y, z): $\begin{pmatrix} n_o^2 & 0 & 0 \\ 0 & n_e^2 & 0 \\ 0 & 0 & n_o^2 \end{pmatrix}$

(z-propagation)

$d_{LN} = 300$ nm,

$\Delta n_e = 0.08$,

$w_{rib} = 0 - 6$ µm, SiO_2 substrate, air cladding

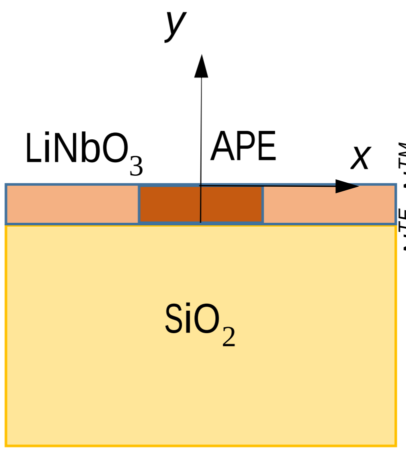

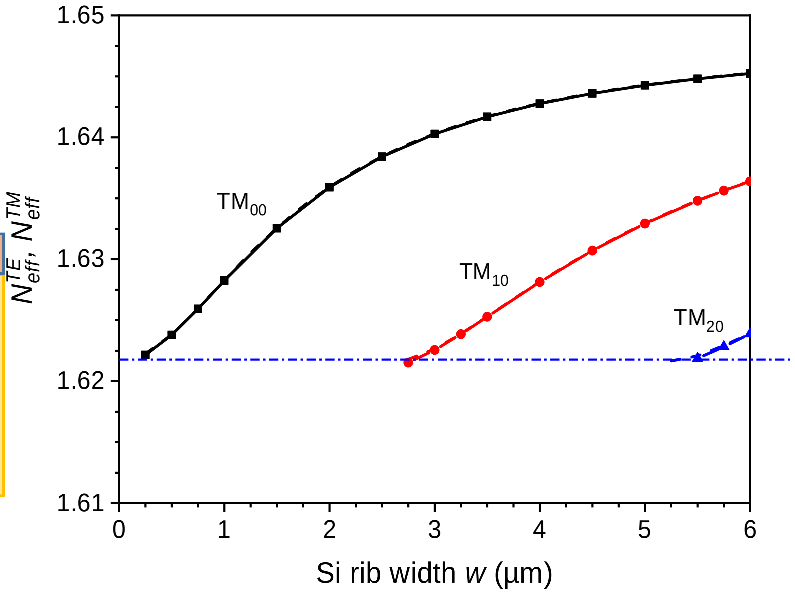

E_y

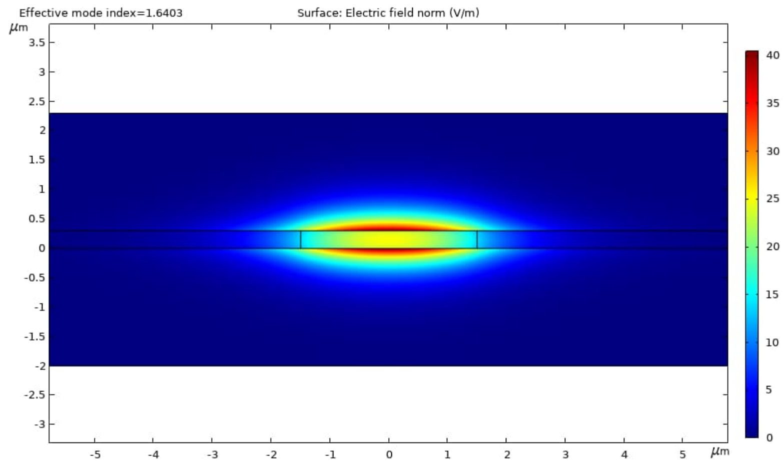

E_x

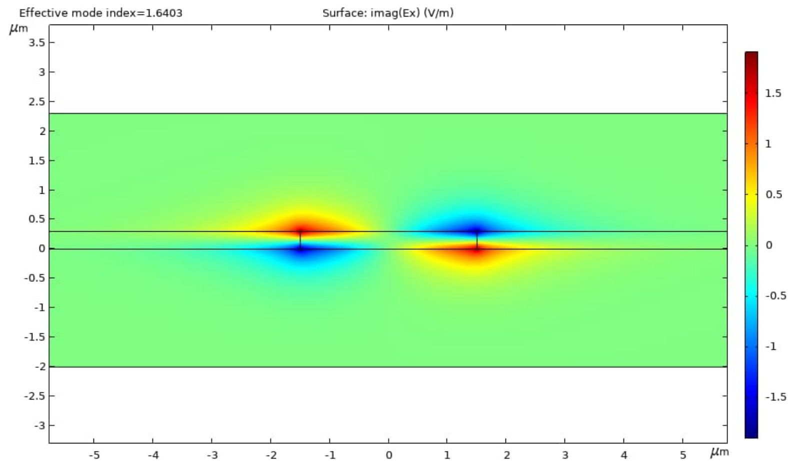

Lossless – but low mode field overlap with $LiNbO_3$ for modulation applications

Asymmetric APE LNOI waveguides – low-loss q-BICs

LN permittivity in coordinates (x, y, z):
(z-propagation)

$$\begin{pmatrix} n_o^2 & 0 & 0 \\ 0 & n_e^2 & 0 \\ 0 & 0 & n_o^2 \end{pmatrix}$$

$$d_{APE\ LN} = 300\text{ nm},\quad d_{tot\ LN} = 500\text{ nm},$$
$$\Delta n_e = 0.08,$$
$$w_{rib} = 0 - 6\ \mu\text{m},$$ SiO_2 substrate, air cladding

E_y

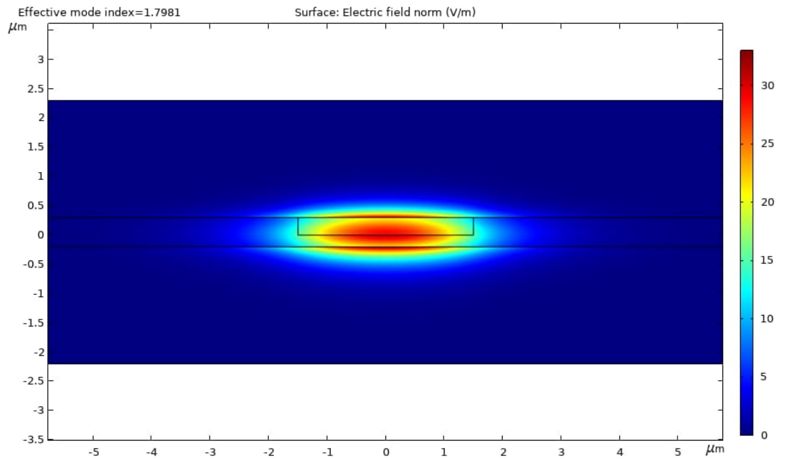

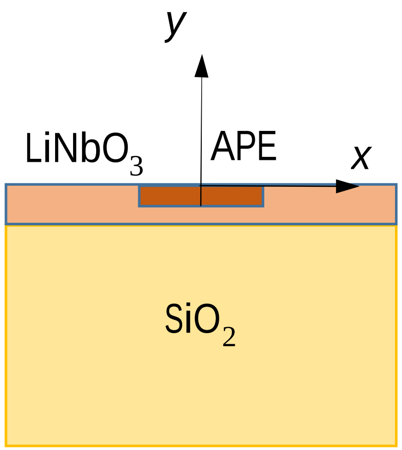

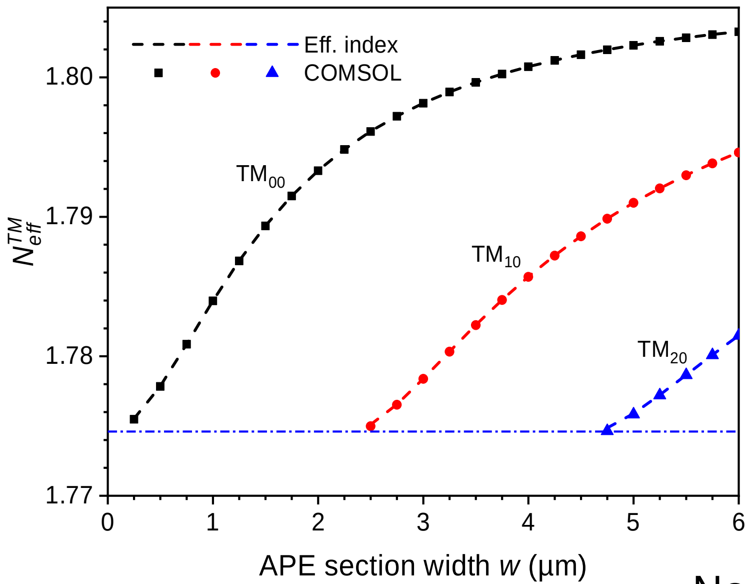

E_x

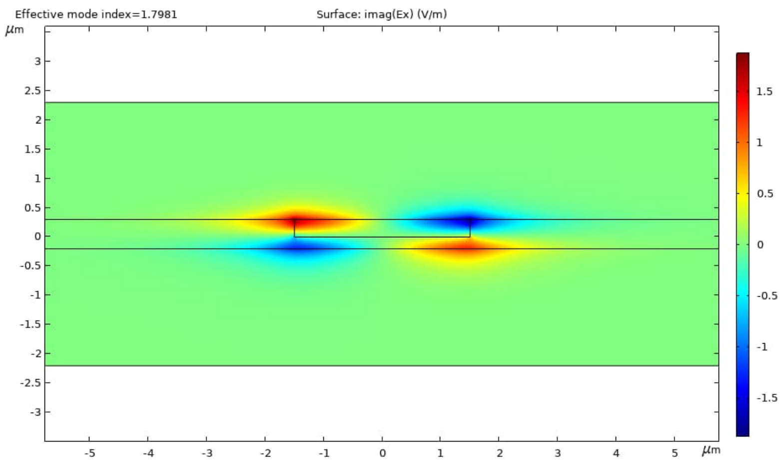

Nonzero but very low loss, high mode field overlap with $LiNbO_3$ for modulation applications

The End